Joint Network Topology and Dynamics Recovery from Perturbed Stationary Points

Hoi-To Wai, Anna Scaglione, Baruch Barzel, Amir Leshem

***Abstract*—This paper presents an inference method to learn a model for complex system based on observations of the perturbed stationary points. We propose to jointly estimate the dynamics parameters and network topology through a regularized regression formulation. A distinguished feature of our approach rests on the direct modeling of *rank deficient* network data, which is widely found in network science but frequently ignored in the prior research. The new modeling technique allows us to provide the *network identifiability* condition under the scenarios of insufficient data. In the special case where the dynamics parameters are known, we show how the interplay between dynamics and sparsity in the graph structure can lead to verifiable conditions for network identifiability. Furthermore, relying only on the steady states equations, our method avoids the necessity to record transient data, and allows to meaningfully combine data from multiple experiments. Numerical experiments are performed on examples with gene regulatory networks and opinion dynamics to justify our claims.**

***Index Terms*—network identification, complex systems, stationary points**

I. Introduction

Our ability to understand and predict the behavior of complex social, biological and technological systems relies on validated mechanistic models that accurately depict the exchanges between their many interacting components. The challenge is that, as opposed to particle and molecular systems, in which interactions are driven by fundamental physical principles [2], [3], the behavior of complex systems is characterized by diverse forms of dynamics, lacking fundamental rules by which to determine the microscopic mechanisms of interactions. For instance, we cannot directly access precise mechanisms of opinion dynamics in social systems, or construct an accurate model for different sub-cellular interactions between genes [4]. To overcome this barrier, we wish to extract the unknown models directly from data — a promising approach that has gained much traction thanks to the proliferation of high throughput data.

Mathematically, a complete model of a complex system includes two layers of descriptions: the *graph structure* (a.k.a. network topology) describing the map of interactions between the components, and the *dynamics* capturing the mechanisms driving these interactions. Using empirical data to learn or recover such complete complex system models is challenging, as the space of potential graphs/mechanisms is vast, and hence its identification requires an infeasible amount of empirical data, casting severe limits on our ability to recover complex system dynamics. In practice, the search space for learning the complex system model can be significantly reduced if we exploit (i) *sparsity* as the majority of relevant systems are characterized by highly sparse graphs; (ii) *prior knowledge* of the network dynamics since for many systems we possess partial knowledge, often heuristic, of the relevant dynamic functions. Prior methods employing the assumptions above are successful in a number of applications; see our literature review in Section I-A.

The main theme of this paper is to show that joint network topology and dynamics parameters recovery can be performed successfully even if one relies only on perturbation data for the stationary points of the system under different conditions. The stationary points are the stable solutions of the steady state equations or the so called *phase portraits* of the system, which can be anticipated in a number of physical systems. For instance, we can measure the stationary point after letting the dynamical system evolves for sufficiently long period of time. We remark that relying on stationary points is advantageous as they are often observed with less noise due to their stationarity over time, e.g., they can be aggregated to reduce variance by repeated experiments. From a theoretical aspect, we investigate a set of *identifiability conditions* under the constraint that the amount of available perturbation data is scarce. This is a common scenario due to the high cost of data acquisition. As a result, the inference problem relies on *rank deficient* data which prohibits perfect recovery of the network topology in general. Despite that, we show here that accurate recovery is achievable under an intertwined condition between the number of edges in the graph and the *expander* property of the graph structure. From a practical aspect, we model the examined complex system using a *parametric template* to fully exploit the prior knowledge on the network dynamics. We describe a family of the relevant models that allows one to develop a tractable inference method for the system's network topology and dynamic parameters.

Overall, our approach provides a data-efficient recipe to infer the system's hidden dynamic equations, capturing its underlying mechanisms, unknown links and their strengths.

Notation. Boldfaced lower-case (*resp.* upper-cased) letters denote vectors (*resp.* matrices) in this paper. For a vector $\boldsymbol{x}$, we use $[\boldsymbol{x}]_i$ or x_i to denote its ith element. We also use $\|\boldsymbol{x}\|$, $\|\boldsymbol{x}\|_1$, $\|\boldsymbol{x}\|_0$, to denote Euclidean norm, ℓ_1 norm and the number of

A preliminary version of this work has been presented at IEEE Data Science Workshop 2018 in Lausanne, Switzerland [1]. HTW is with Dept. of SEEM, The Chinese University of Hong Kong, Hong Kong (htwai@se.cuhk.edu.hk). AS is with School of ECEE, Arizona State University, Tempe, AZ, USA (Anna.Scaglione@asu.edu). BB is with Dept. of Math., Bar-Ilan University, Ramat Gan, Israel (baruchbarzel@gmail.com). AL is with Faculty of Eng., Bar-Ilan University, Ramat Gan, Israel (leshem.amir2@gmail.com).

non-zeros of $\boldsymbol{x}$, respectively. For a matrix $\boldsymbol{X}$, X_{ij} denotes its (i,j)th element whereas $\boldsymbol{x}_i^{\text{row}}$ denotes its ith row vector and $[\boldsymbol{X}]_{\mathcal{I},:}$ denotes the collection of its row vectors in the index set $\mathcal{I}$. Moreover, $\|\boldsymbol{X}\|_F := \|\text{vec}(\boldsymbol{X})\|$ is the Frobenius norm. The operator $\odot$ denotes element-wise product between two vectors/matrices. For any $K \in \mathbb{Z}_+$, we have $[K] := \{1, ..., K\}$.

A. Prior Work

The problem of network topology reconstruction has attracted the interest of many researchers in recent years, and the ideas researched can be coarsely divided in two classes of methodologies. One popular approach is largely agnostic about the family of models, and takes a statistical view of the network identification problem. In addition to heuristics such as thresholding correlation matrices [5] or unsupervised learning [6]–[8], a disciplined method is to impose a graphical model as the latent model to the observed data. We then view the observed data as outcomes of *independent* random experiments. The graphical model captures the conditional independence among state variables, and the graph topology is encoded in the inverse of the data covariance matrix. Further exploiting sparsity of the graph yields the *graphical LASSO problem* [9] — let $\hat{\boldsymbol{C}}$ be the sampled covariance matrix of some observations from the network and $\boldsymbol{A}$ be the estimated adjacency matrix encoding the network topology, we consider

$$\min_{\boldsymbol{A} \succeq \boldsymbol{0}} \; -\log\det \boldsymbol{A} + \text{Tr}(\boldsymbol{A}\hat{\boldsymbol{C}}) + \rho \, \|\text{vec}(\boldsymbol{A})\|_1, \qquad (1)$$

where $\rho \geq 0$ is a penalty parameter controlling sparsity of the solution, as overviewed in [10]. Despite having a well understood performance in terms of consistency and convergence rate [11], the graphical model approach has two fundamental shortcomings: 1) it can identify only undirected graphs; 2) in phenomena that exhibit interesting emergent behavior, the posited model does not capture the network structure — in some cases, sample covariance matrix may even be ill conditioned, leading to severe numerical problems in the identification of the network. In particular, consistency guarantees for graphical LASSO, such as [12], rely on the assumption that $\hat{\boldsymbol{C}}$ converges to $\boldsymbol{A}^{-1}$ as the number of samples accrued goes to infinity. This implicitly requires the ground truth covariance matrix to be a *full rank matrix*, which is not satisfied by a number of the physical phenomenon observed in complex systems. For instance, the set of perturbation data for gene network reconstruction where the observation rank is limited by the amount of data available [13].

Another approach is aware of the model and uses data that correspond to the dynamic evolution during transients in order to solve an inverse optimization problem. This line of work can be found in the physics community employing nonlinear models [14], [15], in inverse optimization [16], in network tomography [17], in parameter estimation [18], [19], as well as the emerging field of graph signal processing exploiting various regularization [20], spectral templates [21], and smoothness with respect to the graph Laplacian [22]–[24], causal modeling [25], [26], model from opinion dynamics [27], structural equation model [28], and joint inference of graph signal with graph topology [29]. There are several benefits coming from this approach. First, this approach captures the causal relationship between the agents interactions, as the network inferred is a directed network. Second, the identification of the non-linearity is expressive of the type of function the agents have in the system. While model mismatch maybe a problem, in most cases reasonable guesses are available; see also the kernel based method in [28]. A disadvantage of this method is its reliance on accurate sampling of data. In some applications sampling transient data is possible, though it may be expensive. In others, the change of state are latent or the states themselves are hidden. An example is the data collected from gene network inference experiments such as [13]. While sampling the data during transients after a perturbation experiment is possible, the data are often noisy and the convergence to stable states is relatively fast, leading to an ill-conditioned problem. Lastly, an underlying assumption of the above methods is that a *sufficient number of snapshots* can be accrued for solving the inverse problem, with an exception for [27], [30], [31] which focus on linear models. The approach in this paper is related to the above methods, but we focus on the *nonlinear* network dynamics inspired by physical systems.

The current paper significantly extended its abridged version [1] by (i) providing complete proofs for the theoretical claims; (ii) performing a unified analysis of identifiability for cases pertaining to dynamical systems; (iii) supporting the claims with extensive empirical analysis.

B. Contributions and Organization

This paper learns a complex system model through observing the *stationary points* generated from it. Our contributions are three-fold. We first formulate a joint recovery problem for the graph structure and dynamics parameter, and we propose a data efficient approach to tackle it. Then, we prove a set of identifiability conditions of the graph structure in a few practical complex system models that are relevant to social and biological networks. We find that these conditions depend upon the graph structure itself, which can be satisfied when the nodes' degrees are roughly constant and small compared to the total number of nodes. Lastly, we demonstrate that the proposed approach achieves outstanding performance on recovering network topology from synthetic and empirical data.

In the remainder of this paper, Section II outlines the proposed models for complex systems and the perturbation experiments for the observed data. Moreover, Section III proposes a computational approach for network dynamics identification, and Section IV provides a set of identifiability guarantees for recovering graph structure from a few relevant models. Lastly, Section V provides case studies on the application of our approach to simulated complex systems and Section VI describes the strategies for processing empirical data.

II. Our Model

The network of interest is described by a strongly connected, directed graph $G = (V, E, \boldsymbol{A})$ with $V = [N] := \{1, ..., N\}$ being the set of N nodes (components) and $E \subseteq V \times V$ is the set of edges that describe the interactions between nodes. If $(j, i) \in E$, it is possible for a change in the state of node j to directly induce changes to the state of node i. The graph is

endowed with a weighted adjacency matrix $\boldsymbol{A} \in \mathbb{R}_+^{N\times N}$ where A_{ij} is the weight of the edge (j,i) and $A_{ij}=0$ if $(j,i)\notin E$. Larger weights mean stronger interactions. Note that self-loops are excluded and therefore $A_{ii}=0$.

In our model, the network dynamics describes the time evolution of the *states* in a complex system as the *superposition of non-linear pairwise interactions*. This can be summarized by the following system of differential equations:

$$\dot{x}_i(t) = g_i(x_i(t)) + \sum_{j=1}^{N} A_{ij} h(x_i(t), x_j(t); \boldsymbol{\theta}_i), \tag{2}$$

for $i=1,...,N$, where $\dot{x}_i(t) := \frac{dx_i(t)}{dt}$ is the first order *time* derivative of the ith node state $x_i(t)$ at time t. In (2), $g_i(\cdot)$ models the self-influence of node i, $\boldsymbol{\theta}_i \in \mathbb{R}^d$ is a set of parameters of the dynamic template functions $h(x,y;\boldsymbol{\theta})$ that model the pairwise state interactions.

Throughout this paper, we assume there exists at least one *non-trivial* stationary point, denoted by $\overline{\boldsymbol{x}} \in \mathbb{R}^N$, to the system (2), and that the system always converges to a stationary point; see [32]. A stationary point $x_i(t)$ satisfies that the right hand side of (2) is zero simultaneously for $i=1,...,N$. To obtain a compact description of the stationary point, it is convenient to define the following vectors:

$$\boldsymbol{a} := \mathrm{vec}(\boldsymbol{A}^\top), \quad \boldsymbol{\theta} := \{\boldsymbol{\theta}_i\}_{i=1}^N, \tag{3}$$

where $\mathrm{vec}(\boldsymbol{A}^\top)$ is the vectorization obtained by stacking up the row vectors of $\boldsymbol{A}$. In the above, $\boldsymbol{a}$ encodes the graph structure and $\boldsymbol{\theta}$ encodes the dynamics parameters for all nodes. We then define the nonlinear response matrix $\boldsymbol{\mathcal{H}}(\boldsymbol{x},\boldsymbol{y};\boldsymbol{\theta})$, whose dimension depends on $\boldsymbol{x},\boldsymbol{y}$, *i.e.,* if $\boldsymbol{x}\in\mathbb{R}^N$, $\boldsymbol{y}\in\mathbb{R}^M$, then $\boldsymbol{\mathcal{H}}(\boldsymbol{x},\boldsymbol{y};\boldsymbol{\theta}) \in \mathbb{R}^{N\times M}$, we have:

$$[\boldsymbol{\mathcal{H}}(\boldsymbol{x},\boldsymbol{y};\boldsymbol{\theta})]_{ij} := h(x_i, y_j; \boldsymbol{\theta}_i), \tag{4}$$

where x_i (*resp.* y_j) is the ith (*resp.* jth) element of the vector $\boldsymbol{x}$ (*resp.* $\boldsymbol{y}$). We additionally define

$$\begin{aligned}\boldsymbol{\mathcal{F}}(\boldsymbol{x},\boldsymbol{y};\boldsymbol{\theta}) &:= \big(\boldsymbol{I}_{N\times N} \otimes \mathbf{1}_M^\top\big)\mathrm{Diag}(\mathrm{vec}(\boldsymbol{\mathcal{H}}^\top(\boldsymbol{x},\boldsymbol{y};\boldsymbol{\theta}))),\\ \boldsymbol{g}(\overline{\boldsymbol{x}}) &:= (g_1(\overline{x}_1),...,g_N(\overline{x}_N))^\top,\end{aligned} \tag{5}$$

where $\otimes$ denotes the Kronecker product and $\mathbf{1}_M$ is an M-dimensional all ones vector. With the definitions above, any stationary point to (2), $\overline{\boldsymbol{x}} := (\overline{x}_1,...,\overline{x}_N)$, satisfies:

$$\mathbf{0} = \boldsymbol{g}(\overline{\boldsymbol{x}}) + \boldsymbol{\mathcal{F}}(\overline{\boldsymbol{x}},\overline{\boldsymbol{x}};\boldsymbol{\theta})\,\boldsymbol{a}. \tag{6}$$

While (6) is non-linear in the state $\overline{\boldsymbol{x}}$, it is linear in the network topology, $\boldsymbol{a}$.

When combined with different *dynamic templates* on the response function $h(\cdot)$, our model in (2) covers a number of common complex systems, as exemplified below.

Example 1 (Gene Dynamics)**.** *Consider a gene regulatory network of N genes. The state $x_i(t)$ is the expression level for the ith gene and the interaction equation (2) dictates how gene is regulated by all other genes*[1]*. The nonlinear dynamics template functions for this case are modeled after the Michaelis-Menten dynamics [33], [34]:*

$$g_i(x) = -x, \quad h(x,y;\boldsymbol{\theta}_i) = h(y;\boldsymbol{\theta}_i) = \frac{y^{\gamma_i}}{1+\delta_i y^{\gamma_i}}, \tag{7}$$

where $\boldsymbol{\theta}_i = (\gamma_i;\delta_i) \in \mathbb{R}_+^2$. A distinctive feature of this dynamics is that the nonlinear function is independent of x. Plugging (7) into (2) shows that the influence from the regulating genes on gene i is independent of the expression level of gene i.

The parameter set consists of two non-negative variables, δ_i and γ_i. When $\delta_i \to 0$, it describes a molecular interaction process which is effectively polynomial in y, hence representing a mass-action kinetic term; when $\delta_i \sim 1$, it describes an activation interaction, in which a gene's regulatory impact saturates to $h(y,\boldsymbol{\theta}_i)\to 1$, capturing the switch-like nature of genetic activation [33]. On the other hand, γ_i controls the diminishing return of the influence strength depending on the expression level of the neighboring gene, such that if γ_i is small, the influence strength will saturate rapidly with increases in the expression levels. See Fig. 1 (left) for an illustration.

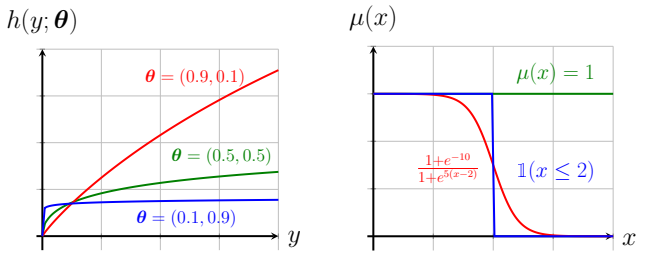

Fig. 1. **Nonlinear Response Functions of Network Dynamics considered**. (Left) The Michaelis-Menten model [cf. (7)]. (Right) Modulation functions of neighbors' opinion effects [cf. (8)].

Example 2 (Opinion Dynamics)**.** *Consider a social network with N agents and edges represent the friendships. The state $x_i(t)$ is the* opinion *of agent i at time t and the interaction equation (2) describes the opinion exchange between agents. The nonlinear dynamics template functions are:*

$$g_i(x) = 0, \;\; h(x,y;\boldsymbol{\theta}_i) = \mu(|y-x|;\boldsymbol{\theta}_i)(y-x), \tag{8}$$

where $\mu(|x|;\boldsymbol{\theta}_i)$ is a non-increasing function in $|x|$ satisfying $\mu(0;\boldsymbol{\theta}_i)=1$.

The non-increasing property of $\mu(|x|;\boldsymbol{\theta}_i)$ modulates the effects of neighbors' opinions that are far away from the agent. Concretely, common examples of $\mu(|x|;\boldsymbol{\theta}_i)$ include —

- ***(a)*** *constant function $\mu_a(|x|)=1$ for all x which is the DeGroot model [35];*
- ***(b)*** *threshold function $\mu_b(|x|;\tau_i) = \mathbb{1}(|x|\le\tau_i)$ which is the bounded confidence model [36];*
- ***(c)*** *sigmoid function $\mu_c(|x|;\tau_i,\sigma_i) = \frac{1+e^{-\sigma_i\tau_i}}{1+e^{\sigma_i(|x|-\tau_i)}}$ which is a smooth approximation of the threshold function.*

*Note the **(a)** is a special case of **(b)** and **(c)** with $\tau_i\to\infty$, and **(b)** can be approximated by **(c)** when $\sigma_i\to\infty$. See Fig. 1 (right) for an illustration of different response functions.*

A. Perturbation Models

The focus of this paper is to identify the *graph structure* and *dynamics* of the complex system (2) using the *stationary points*

[1]Note that a highly expressed gene transcribes proteins at increased rates, leading to a higher concentration level of proteins.

observed from the network dynamics. For convenience, we shall denote the relevant parameters by $\boldsymbol{\Theta} := (\boldsymbol{a}, \boldsymbol{\theta})$. Given the set of stationary points, a natural idea is to recover $\boldsymbol{\Theta}$ through fitting the set of equations (6) defined on the set of stationary points. However, a complex system admits only a few modes of stationary points. In particular, the set of stationary points

$$\overline{\mathcal{X}} := \{\overline{\boldsymbol{x}} \in \mathbb{R}^N \ : \ \boldsymbol{0} = \boldsymbol{g}(\overline{\boldsymbol{x}}) + \boldsymbol{\mathcal{F}}(\overline{\boldsymbol{x}}, \overline{\boldsymbol{x}}; \boldsymbol{\theta})\, \boldsymbol{a}\}, \tag{9}$$

lies in a low dimensional subspace of $\mathbb{R}^N$. For example, if we consider opinion dynamics with a modulating function satisfying $\mu(|x|; \boldsymbol{\theta}) > 0$ for all x [cf. Example 2] and the graph G is strongly connected, then one has $\overline{\mathcal{X}} = \text{span}\{\boldsymbol{1}\}$ [37], *i.e.,* $\overline{\mathcal{X}}$ is a one dimensional subspace of $\mathbb{R}^N$. Under the premise of a low dimensional $\overline{\mathcal{X}}$, recovering $\boldsymbol{\Theta}$ can be challenging, if not impossible, as the latter comprises of at least N^2 parameters and $\overline{\mathcal{X}}$ does not generate a sufficient number of equations for identifying $\boldsymbol{\Theta}$. As a remedy, a common approach adopted by practitioners is to consider adding *perturbations* which produces additional perturbed stationary points to help revealing the network.

We study two types of perturbations, *topological perturbations* and *dynamical perturbations*, of complex systems that are motivated by real experiment setups. Later we shall show that for these types of perturbation, a stationary point $\boldsymbol{x}^{\text{pert}}$ satisfies:

$$\boldsymbol{0} = \boldsymbol{g}^{\text{pert}}(\boldsymbol{x}^{\text{pert}}) + \boldsymbol{\mathcal{F}}^{\text{pert}}(\boldsymbol{x}^{\text{pert}}, \boldsymbol{\theta})\, \boldsymbol{a}, \tag{10}$$

for some $\boldsymbol{g}^{\text{pert}}(\cdot), \boldsymbol{\mathcal{F}}^{\text{pert}}(\cdot)$ that depends on the complex system and perturbation. Similar to a number of prior work [21], [23], [29], we assumed implicitly that the network topology is unchanged upon perturbation. Moreover,

Assumption 1. *The perturbed system converges to one stationary point, for instance, $\boldsymbol{x}^{\text{pert}}$, which satisfies* (10)*.*

Let us study two specific perturbation types in detail —

Topology Perturbations. The topology can be modified in two ways: by eliminating a node and by eliminating an edge.

Node perturbation: Let $\pi(k) \in \{1, ..., N\}$ be a selected node at the kth perturbation. Starting from some time t_0, node $\pi(k)$ is removed from the system in the topology perturbation experiment. The state evolution now obeys

$$\dot{x}_i(t) = g_i(x_i(t)) + \sum_{j=1, j\neq\pi(k)}^{N} A_{ij} h(x_i(t), x_j(t); \boldsymbol{\theta}_i), \tag{11}$$

for $i = 1, ..., \pi(k)-1, \pi(k)+1, ..., N$ and any $t \geq t_0$. Setting the right hand side of (11) to zero, the stationary point $\overline{\boldsymbol{x}}^{(k)}$ satisfies (10) with:

$$\begin{aligned} \boldsymbol{g}^k(\overline{\boldsymbol{x}}^{(k)}) &= (\boldsymbol{I} - \boldsymbol{e}_{\pi(k)}\boldsymbol{e}_{\pi(k)}^\top)\boldsymbol{g}(\overline{\boldsymbol{x}}^{(k)}), \\ \boldsymbol{\mathcal{F}}^k(\overline{\boldsymbol{x}}^{(k)}, \boldsymbol{\theta}) &= (\boldsymbol{I} - \boldsymbol{e}_{\pi(k)}\boldsymbol{e}_{\pi(k)}^\top)\boldsymbol{\mathcal{F}}(\overline{\boldsymbol{x}}^{(k)}, \overline{\boldsymbol{x}}^{(k)}; \boldsymbol{\theta}) \\ &\qquad \text{Diag}\big(\text{vec}(\boldsymbol{1}(\boldsymbol{1} - \boldsymbol{e}_{\pi(k)})^\top)\big), \end{aligned} \tag{12}$$

where $[\boldsymbol{e}_{\pi(k)}]_i = 0$ for $i \neq \pi(k)$, and $[\boldsymbol{e}_{\pi(k)}]_i = 1$ if $i = \pi(k)$. As seen, this perturbation operates on the *topology level*, disconnecting a node from the rest of the network.

This type of perturbation is relevant to gene deletion experiments that are common in gene network recovery [13]. A special case is that with the type of dynamics specified in (7), the effect of topology perturbation on the steady state is equivalent to setting a *boundary condition* on the dynamics such that $x_{\pi(k)}(t) = 0$ and *knocking out* the gene $\pi(k)$.

Edge perturbation : In this case we have $\pi(k) \in E$. It is easy to understand that the structural change affects only $\boldsymbol{\mathcal{F}}^{\text{pert}}(\cdot)$ and the stationary point satisfies (10) with:

$$\begin{aligned} \boldsymbol{g}^k(\overline{\boldsymbol{x}}^{(k)}) &= \boldsymbol{g}(\overline{\boldsymbol{x}}^{(k)}), \\ \boldsymbol{\mathcal{F}}^k(\overline{\boldsymbol{x}}^{(k)}, \boldsymbol{\theta}) &= \boldsymbol{\mathcal{F}}(\overline{\boldsymbol{x}}^{(k)}, \overline{\boldsymbol{x}}^{(k)}; \boldsymbol{\theta})(\boldsymbol{I} - \boldsymbol{e}_{\pi(k)}\boldsymbol{e}_{\pi(k)}^\top). \end{aligned} \tag{13}$$

The perturbation effect can also be captured as a sparse perturbation of the network vector $(\boldsymbol{I} - \boldsymbol{e}_{\pi(k)}\boldsymbol{e}_{\pi(k)}^\top)\boldsymbol{a} = \boldsymbol{a} + \boldsymbol{w}_k$ where $\boldsymbol{w}_k = -\boldsymbol{e}_{\pi(k)} A_{\pi(k)}$. Since in our setting the network is unknown the type of experiment that would lead to such perturbation would have to be blind to what particular edge has been removed. In this case, the inference problem formulation should identify not only $\boldsymbol{a}$ and $\boldsymbol{\theta}$ but also the sparse vector $\boldsymbol{w}_k$ that corresponds to the edge or edges that are deactivated through the perturbation. Given the lack of a specific example or set of data to test these methods, we are going to focus on the node removal in the following.

Dynamics Perturbations. Consider modifying (2) by including external controls into the system. For the kth perturbation experiment, let $u_i^{(k)}(t)$ be the additional control signal applied to the system after $t \geq t_0$. The perturbed system obeys

$$\dot{x}_i(t) = g_i(x_i(t)) + \sum_{j=1}^{N} A_{ij} h(x_i(t), x_j(t); \boldsymbol{\theta}_i) + u_i^{(k)}(t), \tag{14}$$

for all $i = 1, ..., N$ and $t \geq t_0$. Suppose that the control signals reach a steady state as $t \to \infty$ and we denote the steady state as $\boldsymbol{u}^{(k)}(\infty) := (u_1^{(k)}(\infty), ..., u_N^{(k)}(\infty))$. It is easy to observe that $\overline{\boldsymbol{x}}^{(k)}$ is a stationary point to the perturbed system if it satisfies (10) with:

$$\begin{aligned} \boldsymbol{g}^k(\overline{\boldsymbol{x}}^{(k)}) &= \boldsymbol{g}(\overline{\boldsymbol{x}}^{(k)}) + \boldsymbol{u}^{(k)}(\infty), \\ \boldsymbol{\mathcal{F}}^k(\overline{\boldsymbol{x}}^{(k)}, \boldsymbol{\theta}) &= \boldsymbol{\mathcal{F}}\big(\overline{\boldsymbol{x}}^{(k)}, \overline{\boldsymbol{x}}^{(k)}; \boldsymbol{\theta}\big). \end{aligned} \tag{15}$$

As seen, this type of perturbation is applied directly to the nodes, by injecting a control signal that alters the nodes' states, and changes the dynamics by introducing external signals.

A relevant setting to this type of perturbation is the opinion dynamics with insertion of *stubborn agents* whose opinions are constant [27], [38]. In this case, the ith control signal is

$$u_i^{(k)}(t) = \sum_{j=1}^{S} B_{ij} h(x_i(t), z_j^{(k)}; \boldsymbol{\theta}_i), \tag{16}$$

where $z_j^{(k)}$ is the jth stubborn agent's opinion and $[\boldsymbol{B}]_{ij} = B_{ij} \geq 0$ is the bipartite network which connects the stubborn to the non-stubborn agents. In particular, the perturbed steady state obeys a specific structure given by:

Lemma 1. *Consider Example 2 of opinion dynamics. If the kth dynamics perturbation is given by $u_i^{(k)}(t) = \sum_{j=1}^{S} B_{ij} h(x_i(t), z_j^{(k)}; \boldsymbol{\theta}_i)$ for all $t \in \mathbb{R}_+$ with $B_{ij} \geq 0$, then it holds that*

$$\overline{\boldsymbol{x}}^{(k)} = (\text{Diag}(\boldsymbol{A}^{(k)}\boldsymbol{1} + \boldsymbol{B}^{(k)}\boldsymbol{1}) - \boldsymbol{A}^{(k)})^{-1}\boldsymbol{B}^{(k)}\boldsymbol{z}^{(k)}, \tag{17}$$

where we have defined $[\boldsymbol{A}^{(k)}]_{ij} := A_{ij}\,\mu(|\overline{x}_j^{(k)} - \overline{x}_i^{(k)}|)$, *and* $[\boldsymbol{B}^{(k)}]_{ij} := B_{ij}\,\mu(|z_j^{(k)} - \overline{x}_i^{(k)}|)$. *Furthermore, if* $\mu(|x|) = 1$ *for all* x *[DeGroot's case], then* $\boldsymbol{A}^{(k)} = \boldsymbol{A}$ *and* $\boldsymbol{B}^{(k)} = \boldsymbol{B}$.

The proof can be found in Appendix A. The lemma shows that the steady states are determined by the network structure and stubborn agents' opinions.

III. Joint Network Topology and Dynamics Recovery Problem

As each of the perturbed system admits a different set of stationary points, together with the unperturbed stationary point from (6), these lead to a set of stationary points that spans an $(K+1)$-dimensional subspace of $\mathbb{R}^N$ in general. Under the assumption that the right dynamics should lead to the sparsest network, we propose to study the following joint topology and dynamics recovery problem:

$$\min_{\tilde{\boldsymbol{a}}\in\mathbb{R}_+^{N^2},\tilde{\boldsymbol{\theta}}\in\mathbb{R}^{Nd}} \ \|\tilde{\boldsymbol{a}}\|_0 \tag{18a}$$

$$\text{s.t. } \boldsymbol{g}^k(\overline{\boldsymbol{x}}^{(k)}) + \boldsymbol{\mathcal{F}}^k(\overline{\boldsymbol{x}}^{(k)},\tilde{\boldsymbol{\theta}})\tilde{\boldsymbol{a}} = \boldsymbol{0},\ k = 0,...,K, \tag{18b}$$

where $\tilde{\boldsymbol{a}}_i$ denotes the ith block of length N in the vector $\tilde{\boldsymbol{a}}$. We have set $\overline{\boldsymbol{x}}^{(0)} = \overline{\boldsymbol{x}}$ and correspondingly $\boldsymbol{g}^0(\overline{\boldsymbol{x}}^{(0)}) = \boldsymbol{g}(\overline{\boldsymbol{x}})$, $\boldsymbol{\mathcal{F}}^0(\overline{\boldsymbol{x}},\boldsymbol{\theta}) = \boldsymbol{\mathcal{F}}(\overline{\boldsymbol{x}},\overline{\boldsymbol{x}};\boldsymbol{\theta})$. For $k \geq 1$, the functions $\boldsymbol{g}^k(\cdot), \boldsymbol{\mathcal{F}}^k(\cdot)$ were defined in the last section. For topological perturbation, the perturbed nodes $\pi(k)$ for each perturbation is known [cf. (12)]; for dynamical perturbation, the control signal is known [cf. (15)]. We set $\boldsymbol{a} \geq \boldsymbol{0}$ in light of the non-negativities requirements in Section II.

As we will show in Section IV, it can be proven that an optimal solution to problem (18) [or a slightly modified version] recovers the true network structure of the complex system. In particular, we find that in the case of *opinion dynamics under dynamical perturbations*, an optimal solution to (18) matches the true network structure.

On the other hand, the network identification problem for the case of *gene dynamics under topology perturbations* requires a pre-processing step based on the data and solving a modified version of (18). First of all, we consider:

Proposition 1. *Denote* $[\boldsymbol{h}(\boldsymbol{x};\boldsymbol{\theta})]_i := h(x_i;\boldsymbol{\theta}_i)$. *If the* k*th topology perturbation,* i.e., $\overline{\boldsymbol{x}} - \overline{\boldsymbol{x}}^{(k)}$, *is small and* $\|(\boldsymbol{I} - \mathbf{e}_{\pi(k)}\mathbf{e}_{\pi(k)}^\top)\boldsymbol{A}\nabla_{\boldsymbol{x}}\boldsymbol{h}(\overline{\boldsymbol{x}}^{(k)};\boldsymbol{\theta})\|_2 < 1$, *where* $\nabla_{\boldsymbol{x}}\boldsymbol{h}(\overline{\boldsymbol{x}}^{(k)};\boldsymbol{\theta})$ *is the Jacobian*[2] *of the vector function* $\boldsymbol{h}(\boldsymbol{x};\boldsymbol{\theta})$, *then it holds that:*

$$\overline{\boldsymbol{x}} - \overline{\boldsymbol{x}}^{(k)} \approx ([\overline{\boldsymbol{x}}]_{\pi(k)})\boldsymbol{e}_{\pi(k)} + [\overline{\boldsymbol{x}}]_{\pi(k)}\tfrac{\partial h(x;\boldsymbol{\theta})}{\partial x}|_{x=0}\,\boldsymbol{a}^{\text{col}}_{\pi(k)}, \tag{19}$$

where $\boldsymbol{e}_{\pi(k)}$ *is the* $\pi(k)$*th coordinate vector and* $\boldsymbol{a}^{\text{col}}_{\pi(k)}$ *is the* $\pi(k)$*th column vector of* $\boldsymbol{A}$.

The proof can be found in Appendix B, which relies on the first order Taylor expansion of nonlinear equations. The proposition shows that the perturbation caused by removing the $\pi(k)$th node is limited to its one-hop (out)-neighbors. Similar results have been qualitatively observed in [39], [40], and our proposition gives a quantitative account. Proposition 1 motivates us to consider the following set. Let $\eta > 0$, define

$$\mathcal{S}_\eta := \bigcup_{k=1}^{K}\left\{i + \pi(k)(N-1) \,:\, i \in [N],\ \frac{[\overline{\boldsymbol{x}}^{(0)} - \overline{\boldsymbol{x}}^{(k)}]_i}{[\overline{\boldsymbol{x}}^{(0)}]_{\pi(k)}} \leq \eta\right\}, \tag{20}$$

which is a subset of $[N^2]$ of cardinality at most KN. Notice that as $K \ll N$, $\mathcal{S}_\eta$ is an estimate of the positions of zeros in a *small* subset of the true network topology $\boldsymbol{a}$. The above set is then used in a modified problem of (18) which incorporates $\mathcal{S}_\eta$, as follows

$$\min_{\tilde{\boldsymbol{a}}\in\mathbb{R}_+^{N^2},\tilde{\boldsymbol{\theta}}\in\mathbb{R}^{Nd}} \ \|\tilde{\boldsymbol{a}}\|_0 \ \text{ s.t. } \ (18b) \text{ and } [\tilde{\boldsymbol{a}}]_{\mathcal{S}} = \boldsymbol{0}., \tag{21}$$

and we set $\mathcal{S} = \mathcal{S}_\eta$ in the interested case of *gene dynamics and topological perturbation*. Since (18) is a special case of (21) with $\mathcal{S} = \emptyset$, we focus on (21) in the rest of this paper.

An obvious drawback of (21) is that it involves a non-convex objective function due to the ℓ_0 norm. To attain a tractable solution, it is common to consider the ℓ_1 norm relaxation:

$$\begin{aligned}\min_{\tilde{\boldsymbol{a}}\in\mathbb{R}_+^{N^2},\tilde{\boldsymbol{\theta}}\in\mathbb{R}^{Nd}} \quad & J_K(\tilde{\boldsymbol{a}},\tilde{\boldsymbol{\theta}}) + \rho\,\|\tilde{\boldsymbol{a}}\|_1 \\ \text{s.t.} \quad & [\tilde{\boldsymbol{a}}]_{\mathcal{S}} = \boldsymbol{0},\end{aligned} \tag{22}$$

with $\rho > 0$ being a regularization parameter and we defined

$$J_K(\tilde{\boldsymbol{a}},\tilde{\boldsymbol{\theta}}) := \frac{1}{K+1}\sum_{k=0}^{K}\left\|\boldsymbol{g}^k(\overline{\boldsymbol{x}}^{(k)}) + \boldsymbol{\mathcal{F}}^k(\overline{\boldsymbol{x}}^{(k)},\tilde{\boldsymbol{\theta}})\,\tilde{\boldsymbol{a}}\right\|^2.$$

We observe that the first term in the objective function of (22) finds the best fit $\boldsymbol{a},\boldsymbol{\theta}$ to the set of perturbed stationary points in the least square sense. And the recovery condition is improved through the use of the ℓ_1 regularization, $\|\boldsymbol{a}\|_1$, which promotes sparsity in the solution.

Problem (22) is non-convex due to the coupling between $\boldsymbol{\theta}$ and $\boldsymbol{a}$. As a remedy, we adopt a standard alternating optimization approach which cycles between the optimization for $\boldsymbol{a}$ and $\boldsymbol{\theta}$; see Algorithm 1. It is well known that the algorithm converges to a stationary point of (22), e.g.,

Algorithm 1 Alternating optimization procedure for (22).

1: **Input**: data $\{\overline{\boldsymbol{x}}^{(k)}\}_{k=1}^K$, initial guess of parameter $\{\boldsymbol{\theta}_i^{(1)}\}_{i=1}^N$, (optional) knowledge on topology from pre-processing, $\mathcal{S}$.
2: **for** $\ell = 1, 2, ...$ **do**
3: Update the estimate on the network topology parameter:

$$\boldsymbol{a}^{(\ell+1)} \in \arg\min_{\tilde{\boldsymbol{a}}\in\mathbb{R}_+^{N^2}} \ J_K(\tilde{\boldsymbol{a}},\boldsymbol{\theta}^{(\ell)}) + \rho\,\|\tilde{\boldsymbol{a}}\|_1 \text{ s.t. } [\tilde{\boldsymbol{a}}]_{\mathcal{S}} = \boldsymbol{0}.$$

4: Update the estimate on dynamics parameter:

$$\boldsymbol{\theta}^{(\ell+1)} \in \arg\min_{\tilde{\boldsymbol{\theta}}\in\mathbb{R}^{Nd}} \ J_K(\boldsymbol{a}^{(\ell+1)},\tilde{\boldsymbol{\theta}}),$$

where the above may be solved using a grid search, or solved inexactly via a projected gradient descent step.
5: **end for**
6: **Output**: estimated network topology and parameters $\boldsymbol{a}^{(\ell+1)}, \boldsymbol{\theta}^{(\ell+1)}$.

[2]The Jacobian is the diagonal matrix $\nabla_{\boldsymbol{x}}\boldsymbol{h}(\overline{\boldsymbol{x}}^{(k)};\boldsymbol{\theta}) := \text{Diag}([..., \partial h(x;\boldsymbol{\theta}_i)/\partial x|_{x=\overline{x}_i^{(k)}}, ...])$.

Proposition 2. *[41, Theorem 2(a)] Every limit point of the sequence* $\{\boldsymbol{a}^{(\ell)}, \boldsymbol{\theta}^{(\ell)}\}_{\ell=1}^{\infty}$ *generated by Algorithm 1 is a stationary point of* (22)*.*

The convergence result also holds when the exact minimization of $\boldsymbol{a}$ or $\boldsymbol{\theta}$ is replaced by a gradient descent sub-routine for further complexity savings; see [41] for instance.

IV. Identifiability of the Network Topology

This section is devoted to studying conditions under which (21) identifies the graph structure that is characterized by the (vectorized) adjacency matrix $\boldsymbol{a}$. We focus on the case when the dynamics parameters $\boldsymbol{\theta}$ are perfectly known. For simplifying notations, throughout this section we shall drop the dependence on $\boldsymbol{\theta}$ of the matrices defined previously.

To begin, observe from (18b) that the equality constraints are equivalent to a set of linear constraints on the parameter $\boldsymbol{a}$. With the aid of sparsity, we can derive a sufficient condition for the perfect recovery of $\boldsymbol{a}$ as follows:

Definition 1. *[42] For a matrix* $\boldsymbol{A}$, $\mathrm{spark}(\boldsymbol{A})$ *(a.k.a. Kruskal rank) is defined as the minimum number* k *such that there exists* k *column vectors of* $\boldsymbol{A}$ *which are linearly dependent.*

Lemma 2. *If it holds that* $K \geq \|\boldsymbol{a}\|_0$ *and*

$$\mathrm{spark}\Big(\Big(\ \boldsymbol{\mathcal{F}}^1\big(\overline{\boldsymbol{x}}^{(1)}\big)^\top\ \cdots\ \boldsymbol{\mathcal{F}}^K\big(\overline{\boldsymbol{x}}^{(K)}\big)^\top\ \Big)^\top\Big) \geq 2K+1, \tag{23}$$

then $\boldsymbol{a}$ *is identifiable via solving* (21) *when* $\boldsymbol{\theta}$ *is known.*

The proof is standard and can be found in Appendix C. The above condition, which is similar to a recent work [29, Theorem 1 & 2], is applicable to arbitrary dynamics under the perturbation models described. However, as the 'spark' of the matrix in (23) is tied directly to topological and non-linear features of the complex networks model, it can be hard to evaluate the condition. The statement of Lemma 2 rings hollow as it is not amenable to interpretation.

Rather than merely relying on Lemma 2, a key challenge of the current work is to demonstrate that knowledge of the underlying dynamical systems in networks enables one to derive interpretable conditions for identifiability. In particular, we shall focus on two special cases, namely **(a)** the gene dynamics with topology perturbations and **(b)** the opinion dynamics with dynamic perturbations.

For case **(a)** with gene dynamics, let $\mathcal{S}_i$ be the restriction of $\mathcal{S}_\eta$ to entries of the ith row vector, $\boldsymbol{a}_i^{\mathrm{row}}$, of $\boldsymbol{A}$ with respect to the vectorized adjacency $\boldsymbol{a}$. We consider

Assumption 2. *The index set* $\mathcal{S}_i$ *is a superset of the set of all zeros in the partial ground truth topology* $[\boldsymbol{a}_i^{\mathrm{row}}]_{\pi([K])}$.

This assumption holds when the approximation in Proposition 1 is accurate, e.g., when the function $h(x)$ in Example 1 is well approximated by a linear function within the operating region. Our main identifiability result is as follows:

Theorem 1. *Under Assumption 2 and let* $\hat{\boldsymbol{a}}$ *be an optimal solution to* (21)*. Fixing* d *and let* $N \to \infty$*. Let the network be a* d-regular random graph*, and* $|\mathcal{S}_i| = \mathcal{O}(1)$ *for all* i*.*

If the perturbation data is observed from $K = \Omega(d)$ *experiments, then it holds in high probability that*

$$\|\hat{\boldsymbol{a}}_i^{\mathrm{row}} - \boldsymbol{a}_i^{\mathrm{row}}\|_1 = \mathcal{O}(\epsilon^{\mathsf{gene}}),\ i = 1, ..., N, \tag{24}$$

where $\boldsymbol{a}_i^{\mathrm{row}}$ (resp. $\hat{\boldsymbol{a}}_i^{\mathrm{row}}$) *refers to the* i*th row of* $\boldsymbol{A}$ (resp. $\hat{\boldsymbol{A}}$)*, for some* $\epsilon^{\mathsf{gene}} > 0$ *modeling the approximation error which is small when the dynamics is roughly linear.*

For case **(b)** with opinion dynamics, we consider

Assumption 3. *The function* μ *in Example 2 satisfies* $\mu(x) \geq 1 - \epsilon^{\mathsf{op}}$ *for all* x*, for some small* $\epsilon^{\mathsf{op}} \in [0, 1]$.

This assumption implies that the nonlinear opinion dynamics is a slightly perturbed version of linear DeGroot dynamics [recall that the latter case has $\mu(x) = 1$ for all x]. We show:

Theorem 2. *Under Assumption 3 and let* $\hat{\boldsymbol{a}}$ *be an optimal solution to* (21)*. Let* d_{max} *be the maximum in-degree of the graph* G *and it is a fixed number,* $N \to \infty$*, and the network (corresponding to* $\boldsymbol{B}$*) between stubborn and non-stubborn agents be such that each non-stubborn agent is connected to exactly* ℓ *stubborn agent, chosen uniformly at random.*

If there are $S = \Omega(d_{\mathsf{max}})$ *stubborn agents and the number of stationary points collected is* $K = S$*, then it holds that*

$$\|\hat{\boldsymbol{a}}_i^{\mathrm{row}} - \boldsymbol{a}_i^{\mathrm{row}}\|_1 = \mathcal{O}(\epsilon^{\mathsf{op}}),\ i = 1, ..., N, \tag{25}$$

where $\boldsymbol{a}_i^{\mathrm{row}}$ (resp. $\hat{\boldsymbol{a}}_i^{\mathrm{row}}$) *is the* i*th row of* $\boldsymbol{A}$ (resp. $\hat{\boldsymbol{A}}$)*, in high probability.*

In both cases, our results show that identifiability depends on the structure of the network to be inferred. This is reasonable as the latter determines the stationary points used as evidence for network inference. In particular, these conditions favor networks whose sub-network has regular degrees. Under these assumptions on the network structure, the theorems guarantee that one can recover the network under the usual condition that the number of stationary points observed K grow with the network's degree. Let us present a general roadmap for the proofs of the theorems.

Roadmap of Analysis. In the first step [cf. Section IV-A], we reduce the identifiability conditions of (21) for case **(a)** and **(b)** into algebraic conditions pertaining to sparse recovery. We show that any solution to (18), $\widetilde{\boldsymbol{a}}_i^{\mathrm{row}}$, must satisfy:

$$\boldsymbol{\Delta}_i = \boldsymbol{\mathcal{E}}_i\big(\boldsymbol{a}_i^{\mathrm{row}} - \widetilde{\boldsymbol{a}}_i^{\mathrm{row}}\big), \tag{26}$$

where $\boldsymbol{\Delta}_i$ is a vector modeling the approximation error, and $\boldsymbol{a}_i^{\mathrm{row}}$ is the ith row vector of $\boldsymbol{A}$. Moreover, $\boldsymbol{\mathcal{E}}_i$ is the weighted adjacency matrix of a bipartite sub-graph taken from the graph to be identified itself.

The second step in Section IV-B is to analyze the properties of $\boldsymbol{\mathcal{E}}_i$ leading to identifiability, *i.e.,* any $\tilde{\boldsymbol{a}}_i^{\mathrm{row}}$ satisfying (26) is $\tilde{\boldsymbol{a}}_i^{\mathrm{row}} \approx \boldsymbol{a}_i^{\mathrm{row}}$. A common feature of our results is that recoverability can be guaranteed when the corresponding sub-graph is a 'good' *expander* —

Definition 2. *A bipartite graph* $G(A, B)$ *with* $|A| = n, |B| = m$ *and* $m \leq n$*, has the expander parameters* $(d_l, d_u, \alpha, \delta)$ *if:*

- *the degrees for the left node set,* A*, are bounded in* $[d_l, d_u]$ *for all* $v_i \in A$*.*

- *for any $S \subseteq A$ with $|S| \leq \alpha n$, we have $\delta|E(S,B)| \leq |N(S)|$, where $E(S,B)$ is the set of edges from S to B and $N(S) = \{v_j \in B : \exists\ v_i \in S\ s.t.\ (v_j, v_i) \in E\}$ is the neighborhood of S in B.*

A 'good' expander has $d_l \approx d_u$, $\delta \approx 1$ and large α. As observed by [43], this is a structural property that can be satisfied by a number of random graph constructions. Concretely, we show that a random construction satisfies the expander requirement in high probability whenever $K = \Omega(d_{\mathsf{max}})$, where d_{max} is the *maximum in-degree of the graph*, thereby establishing the identifiability of the network weights when the number of perturbation experiments is sufficient (proportional to the density of the graph).

Lastly, the final step in Section IV-C proves the theorems by using the condition for the existence of expander graphs and compare it with the random graph models assumed for the graphs of interest.

Remark 1. *The Assumptions 2, 3 required are indeed stringent. One may question about their validity in more practical nonlinear dynamics. For this, we shall relegate the examination of the sensitivity of network inference method to our empirical analysis. That said, the importance of our results is to provide a guideline for designing network inference experiments via an interpretable identifiability condition.*

A. Step 1: Problem Reduction

Below, we show that the solution to (21) can be written in the form of (26) for case **(a)** and **(b)**.

Case (a): Gene Dynamics with Topology Perturbations. We assume that $\pi(k) = k$ without loss of generality. Using structure of the Kronecker products, we can decompose (21) into N sub-problems that to be considered independently. For $i = 1, ..., N$, consider

$$\hat{\boldsymbol{a}}_i^{\text{row}} \in \underset{\tilde{\boldsymbol{a}}_i^{\text{row}} \in \mathbb{R}_+^N}{\arg\min} \quad \|\tilde{\boldsymbol{a}}_i^{\text{row}}\|_0 \tag{27a}$$

$$\text{s.t. } [\tilde{\boldsymbol{a}}_i^{\text{row}}]_{\mathcal{S}_i} = \boldsymbol{0}, \tag{27b}$$

$$[\overline{\boldsymbol{x}}^{(k)}]_i = (\boldsymbol{a}_i^{\text{row}})^\top \boldsymbol{h}(\overline{\boldsymbol{x}}^{(k)}),\ k = 0, 1, ..., K. \tag{27c}$$

Following the insights from Lemma 2, we observe that an identifiability condition for (27) depends on the steady states $\overline{\boldsymbol{x}}^{(k)}$, $k = 1, ..., K$. The main challenge, however, lies on the fact that the steady state $\overline{\boldsymbol{x}}^{(k)}$ is generated from a nonlinear system which is not available in a closed form. To tackle the issue, we resort to a Taylor approximation approach which unveils a critical relationship between identifiability using (27) and the structure of network topology.

Denote the set of K-dimensional vectors $\{\boldsymbol{y}_i\}_{i=1}^N$ given by $[\boldsymbol{y}_i]_k := [\overline{\boldsymbol{x}}^{(k)}]_i - \overline{x}_i$, $k = 1, ..., K$. Observe that $[\overline{\boldsymbol{x}}^{(k)}]_i = (\boldsymbol{a}_i^{\text{row}})^\top \boldsymbol{h}(\overline{\boldsymbol{x}}^{(k)})$, when $i \notin [K]$, it holds

$$\begin{aligned}[\boldsymbol{y}_i]_k &= (\boldsymbol{a}_i^{\text{row}})^\top \big(\boldsymbol{h}(\overline{\boldsymbol{x}}^{(k)}) - \boldsymbol{h}(\overline{\boldsymbol{x}})\big) \\ &\approx \overline{x}_k\, (\boldsymbol{a}_i^{\text{row}})^\top \text{Diag}(\overline{\boldsymbol{h}}')\big(\tfrac{\partial h(x)}{\partial x}|_{x=0}\, \boldsymbol{a}_k^{\text{col}} + \mathbf{e}_k\big),\end{aligned} \tag{28}$$

where $[\overline{\boldsymbol{h}}']_i := \frac{\partial h(x)}{\partial x}|_{x=\overline{x}_i^{(k)}}$. The approximation above is due to Proposition 1 and applying the Taylor approximation on the difference vector $\boldsymbol{h}(\overline{\boldsymbol{x}}) - \boldsymbol{h}(\overline{\boldsymbol{x}}^{(k)})$. Stacking up (28) from $k = 1$ to $k = K$, we obtain the linear system:

$$\boldsymbol{y}_i \approx \boldsymbol{\Lambda}\big(\big(\boldsymbol{I}_{K\times K} \quad \boldsymbol{0}_{K\times(N-K)}\big) + \tilde{\boldsymbol{E}}_i\big)\, \text{Diag}(\overline{\boldsymbol{h}}')\, \boldsymbol{a}_i^{\text{row}}, \tag{29}$$

where we have defined

$$\tilde{\boldsymbol{E}}_i := \tfrac{\partial h(x)}{\partial x}|_{x=0}\big([\boldsymbol{A}]_{:,[K]}\big)^\top \quad \text{and} \quad \boldsymbol{\Lambda} := \text{Diag}(\overline{\boldsymbol{x}}). \tag{30}$$

Applying a similar set of approximations to the equalities in (27c) implies

$$\begin{aligned}&\boldsymbol{y}_i \approx \boldsymbol{\Lambda}\Big(\big(\boldsymbol{I}_{K\times K} \quad \boldsymbol{0}_{K\times(N-K)}\big) + \tilde{\boldsymbol{E}}_i\Big)\, \text{Diag}(\overline{\boldsymbol{h}}')\, \tilde{\boldsymbol{a}}_i^{\text{row}} \\ &(\text{as } \boldsymbol{\Lambda} \neq \boldsymbol{0}) \Longrightarrow \\ &\boldsymbol{0} \approx \Big(\big(\boldsymbol{I}_{K\times K} \quad \boldsymbol{0}_{K\times(N-K)}\big) + \tilde{\boldsymbol{E}}_i\Big)\, \text{Diag}(\overline{\boldsymbol{h}}')\, \big(\tilde{\boldsymbol{a}}_i^{\text{row}} - \boldsymbol{a}_i^{\text{row}}\big).\end{aligned} \tag{31}$$

Eq. (31) characterizes the restriction on the optimization variable $\tilde{\boldsymbol{a}}_i^{\text{row}}$ implied by the constraint Eq. (27c), which is an underdetermined system as $N \gg K$. The matrix inside the bracket on the right hand side of (31) can be regarded as a *sensing matrix* for the system. As the identity matrix $\boldsymbol{I}$ tends to have a larger magnitude than $\tilde{\boldsymbol{E}}_i$, the overall sensing matrix $(\boldsymbol{I}\ \boldsymbol{0}) + \tilde{\boldsymbol{E}}_i$ will be dominated by $\boldsymbol{I}$. That is, $(\boldsymbol{I}\ \boldsymbol{0}) + \tilde{\boldsymbol{E}}_i \approx (\boldsymbol{I}\ \boldsymbol{0})$. This implies that the elements of $\boldsymbol{a}_i^{\text{row}}$ over the coordinates $[N] \setminus [K]$ can be unrecoverable as the rows of the sensing matrix are (approximately) supported only on $[K]$.

Let us utilize the constraint (27b) to refine our conditions. Under Assumption 2, the matrix-vector product on the right hand side of (31) evaluates to zero for the rows in $\mathcal{S}_i$. Importantly, it implies

$$\boldsymbol{\Delta}_i^{\mathsf{gene}} = \boldsymbol{E}_i\, \big(\tilde{\boldsymbol{a}}_i^{\text{row}} - \boldsymbol{a}_i^{\text{row}}\big) \text{ where } \boldsymbol{E}_i := \big[\tilde{\boldsymbol{E}}_i\big]_{\mathcal{S}_i,:}\text{Diag}(\overline{\boldsymbol{h}}'), \tag{32}$$

and $\boldsymbol{\Delta}_i^{\mathsf{gene}}$ with $\|\boldsymbol{\Delta}_i^{\mathsf{gene}}\|_1 \leq \epsilon^{\mathsf{gene}}$ models the overall approximation error due to the approximations used. This retrieves a similar form as (26). Therefore, Eq. (32) now corresponds to a *reduced* identifiability condition that depends on $\boldsymbol{E}_i$ which itself is a sub-graph of the graph to be identified.

Case (b): Opinion Dynamics with Dynamics Perturbations from Stubborn Agents. For any i, k, define the total influence strength on the agents [cf. (17)] as

$$c_i^{(k)} := \boldsymbol{1}^\top(\boldsymbol{\mu}_{A,i}^{(k)} \odot \boldsymbol{a}_i^{\text{row}}) + \boldsymbol{1}^\top(\boldsymbol{\mu}_{B,i}^{(k)} \odot \boldsymbol{b}_i^{\text{row}}), \tag{33}$$

where $\boldsymbol{\mu}_{A,i}^{(k)}$ (*resp.* $\boldsymbol{\mu}_{B,i}^{(k)}$) is a vector whose jth element equals $\mu(|\overline{x}_i^{(k)} - \overline{x}_j^{(k)}|)$ [*resp.* $\mu(|z_j^{(k)} - \overline{x}_i^{(k)}|)$]. We assume that $c_i^{(k)} > 0$ for any i, k and the normalized control signal's value $u_i^{(k)}/c_i^{(k)}$ is known.

Similar to the development of (27) and by setting $M_i \geq \max_k c_i^{(k)}$, we observe that solving (21) is equivalent to solving the sub-problems for $i = 1, ..., N$,

$$\begin{aligned}\min_{\tilde{\boldsymbol{a}}_i^{\text{row}} \in \mathbb{R}_+^N} \ & \|\tilde{\boldsymbol{a}}_i^{\text{row}}\|_0 \\ \text{s.t. } & (\overline{\boldsymbol{x}}^{(k)})^\top\big(\boldsymbol{\mu}_i^{(k)} \odot \tilde{\boldsymbol{a}}_i^{\text{row}}\big) = \overline{x}_i^{(k)} - u_i^{(k)}/c_i^{(k)}, \\ & [\tilde{\boldsymbol{a}}_i^{\text{row}}]_i = 0,\ \|\tilde{\boldsymbol{a}}_i^{\text{row}}\|_1 \leq M_i,\ k \in [K],\end{aligned} \tag{34}$$

Again, our challenge is to study the feasible set of (34) through explicitly modeling the stationary points.

Applying (15) and Lemma 1 show that for all $k = 1, ..., K$,

$$\overline{x}_i^{(k)} c_i^{(k)} - u_i^{(k)} = (\boldsymbol{B}^{(k)} \boldsymbol{z}^{(k)})^\top (\boldsymbol{I} - \mathrm{Diag}(\boldsymbol{c}^{(k)})^{-1} \boldsymbol{A}^{(k)})^{-\top} (\boldsymbol{\mu}_i^{(k)} \odot \boldsymbol{a}_i^{\mathrm{row}}), \tag{35}$$

where the ith element of $\boldsymbol{c}^{(k)}$ is $c_i^{(k)}$. Consequently, using (17), any feasible solution $\tilde{\boldsymbol{a}}_i^{\mathrm{row}}$ to (34) must satisfy

$$0 = (\boldsymbol{B}^{(k)} \boldsymbol{z}^{(k)})^\top (\boldsymbol{I} - \mathrm{Diag}(\boldsymbol{c}^{(k)})^{-1} \boldsymbol{A}^{(k)})^{-\top} (\boldsymbol{\mu}_i^{(k)} \odot (\boldsymbol{a}_i^{\mathrm{row}} - \tilde{\boldsymbol{a}}_i^{\mathrm{row}})), \tag{36}$$

for all $k = 1, ..., K$. Define the matrices $\mathsf{U}_B^{(k)}, \mathsf{U}_A^{(k)}$,

$$[\mathsf{U}_B^{(k)}]_{ij} = \mu(|z_j^{(k)} - \overline{x}_i^{(k)}|), \ [\mathsf{U}_A^{(k)}]_{ij} = \mu(|\overline{x}_j^{(k)} - \overline{x}_i^{(k)}|). \tag{37}$$

Observe the decompositions:

$$\begin{aligned} \boldsymbol{B}^{(k)} &= \boldsymbol{B} + \delta \boldsymbol{B}^{(k)}, \ \delta \boldsymbol{B}^{(k)} := (\mathsf{U}_B^{(k)} - \boldsymbol{1}\boldsymbol{1}^\top) \odot \boldsymbol{B} \\ \boldsymbol{A}^{(k)} &= \boldsymbol{A} + \delta \boldsymbol{A}^{(k)}, \ \delta \boldsymbol{A}^{(k)} := (\mathsf{U}_A^{(k)} - \boldsymbol{1}\boldsymbol{1}^\top) \odot \boldsymbol{A}, \end{aligned} \tag{38}$$

where we notice that $\|\delta \boldsymbol{A}^{(k)}\| = \mathcal{O}(\epsilon^{\mathsf{op}}), \|\delta \boldsymbol{B}^{(k)}\| = \mathcal{O}(\epsilon^{\mathsf{op}})$ due to Assumption 3.

For small ϵ^{op}, using the above decomposition shows that (36) is equivalent to

$$(\boldsymbol{z}^{(k)})^\top \big(\boldsymbol{B}^\top (\boldsymbol{I} - \mathrm{Diag}(\boldsymbol{c})^{-1} \boldsymbol{A})^{-1} + \boldsymbol{\zeta}^{(k)}\big)(\boldsymbol{a}_i^{\mathrm{row}} - \tilde{\boldsymbol{a}}_i^{\mathrm{row}}) = \boldsymbol{0}, \tag{39}$$

where $\|\boldsymbol{\zeta}^{(k)}\| = \mathcal{O}(\epsilon^{\mathsf{op}})$ and $\boldsymbol{c}$ is a vector whose ith element equals $\boldsymbol{1}^\top \boldsymbol{a}_i^{\mathrm{row}} + \boldsymbol{1}^\top \boldsymbol{b}_i^{\mathrm{row}}$. Assume $\boldsymbol{Z}$ is full row rank and $K = S$, where the number of perturbation experiments equals the number of stubborn agents. Concatenating the K constraints in (39) and using the boundedness of $\tilde{\boldsymbol{a}}_i^{\mathrm{row}}, \boldsymbol{a}_i^{\mathrm{row}}$ show

$$\boldsymbol{\Delta}_i^{\mathsf{op}} = \boldsymbol{B}^\top (\boldsymbol{I} - \mathrm{Diag}(\boldsymbol{c})^{-1} \boldsymbol{A})^{-\top} (\boldsymbol{a}_i^{\mathrm{row}} - \tilde{\boldsymbol{a}}_i^{\mathrm{row}}), \tag{40}$$

where in this case $\|\boldsymbol{\Delta}_i^{\mathsf{op}}\| = \mathcal{O}(\epsilon^{\mathsf{op}})$ models the error due to nonlinearity. In particular, we will show that $\boldsymbol{B}^\top$ in (40) plays a similar role as $\boldsymbol{E}_i$ found in (32).

B. Step 2: Identifiability Condition with Expander Graphs

The next step is to examine a common condition on $\boldsymbol{E}_i$ and $\boldsymbol{B}^\top$ for (32) and (40) to ensure that $\tilde{\boldsymbol{a}}_i^{\mathrm{row}} \approx \boldsymbol{a}_i^{\mathrm{row}}$ in the network topology identification problems. In particular, the support of $\boldsymbol{E}_i$ coincides with the partial adjacency matrix $\boldsymbol{A}_{:,\mathcal{S}_i}^\top$; while the support of $\boldsymbol{B}^\top$ coincides with the sub-graph connecting between the stubborn and non-stubborn agents. The support of these matrices can be described by a bipartite graph $G_i(A, B)$ where A with $|A| = N$ is denoted by convention as the left node set, and B with $|B| = |\mathcal{S}_i|$ (for $\boldsymbol{E}_i$), or $|B| = S$ (for $\boldsymbol{B}^\top$) is denoted as the right node set. The edge set of $G_i(A, B)$ is given as:

$$E(G_i(A, B)) := \big\{(\ell, q) : \ell \in A, q \in B, \big[\boldsymbol{\mathcal{E}}\big]_{q,\ell} \neq 0\big\}, \tag{41}$$

where we set $\boldsymbol{\mathcal{E}} = \boldsymbol{E}_i$ for the gene dynamics, and $\boldsymbol{\mathcal{E}} = \boldsymbol{B}^\top$ for the opinion dynamics. Our first observation lies in the following proposition which connects the structure of $G_i(A, B)$ to the identifiability of $\boldsymbol{a}_i^{\mathrm{row}}$ from (32) and (40):

Proposition 3. *Consider the bipartite graph $G_i(A, B)$ described in (41) and the sensing matrix $\boldsymbol{\mathcal{E}}$. Let $G_i(A, B)$ be an $(d_l, d_u, \alpha, \delta)$ expander graph [see Definition 2]. For any $1 \leq s \leq |\mathcal{S}_i|$, if $2s \leq \alpha N$, and the entries of $\boldsymbol{\mathcal{E}}$ satisfy*

$$\begin{aligned} &e_{\mathsf{min}}\, \delta d_l - e_{\mathsf{max}}(d_u - \delta d_l) > 0, \\ &e_{\mathsf{max}} := \max_{\ell,q} \ [\boldsymbol{\mathcal{E}}]_{\ell,q}, \ e_{\mathsf{min}} := \min_{\ell,q, \ [\boldsymbol{\mathcal{E}}]_{\ell,q} \neq 0} \ [\boldsymbol{\mathcal{E}}]_{\ell,q}. \end{aligned} \tag{42}$$

Then, for all vector $\boldsymbol{x} \in \mathbb{R}^N$ with $\|\boldsymbol{x}\|_0 \leq 2s$, it holds that

$$\|\boldsymbol{\mathcal{E}}\boldsymbol{x}\|_1 \geq \upsilon^\star \|\boldsymbol{x}\|_1, \ \textit{where} \ \upsilon^\star := e_{\mathsf{min}}\, \delta d_l - e_{\mathsf{max}}(d_u - \delta d_l). \tag{43}$$

The proof can be found in Appendix D. The proposition shows that if G_i is a 'good' expander (with $d_u \approx d_l$, $\delta \approx 1$ and large α) such that the conditions in (42) are satisfied, then the sparse matrix $\boldsymbol{\mathcal{E}}$ satisfies a one-sided restricted isometry property (RIP) with an order proportional to αN.

We next characterize the expander graph parameters of the induced graph $G_i(A, B)$ [cf. (41)] to satisfy (42), with a focus on the interplay between the number of perturbations K and the sparsity of the unknown $\boldsymbol{a}_i^{\mathrm{row}}$. To this end, we borrow the following proposition from our previous work:

Proposition 4. *[27, Proposition 5] Let $G(A, B)$ be a bigraph with $|A| = N$, $|B| = \beta^\star N$, and its degree sequence is fixed for the left node set as $d(v_i)$. Denote $d_l = \min_{i \in A} d(v_i)$ and $d_u = \max_{i \in A} d(v_i)$. Suppose the edge set of $G(A, B)$ is generated such that for each $v_i \in A$, we connect the node to $d(v_i)$ random neighbors in B uniformly. Fix $\alpha \in (0, 1)$ and set*

$$\beta^\star > \inf \Big\{\beta \in (0, 1) : \beta > \alpha, \ d_l > \max\Big\{3, \frac{H(\alpha) + \beta H(\alpha/\beta)}{\alpha \log(\beta/\alpha)}\Big\}\Big\}, \tag{44}$$

where $H(\alpha) = \alpha \log \alpha + (1 - \alpha) \log(1 - \alpha)$ is the binary entropy function. Then, with high probability as $N \to \infty$, the graph $G(A, B)$ is an $(d_l, d_u, \alpha, 1 - \frac{1}{d_l})$-expander.

	$\alpha = 0.08$	$\alpha = 0.16$	$\alpha = 0.24$	$\alpha = 0.32$
$d_l = 4$	$\beta \geq 0.342$	$\beta \geq 0.528$	$\beta \geq 0.673$	$\beta \geq 0.794$
$d_l = 5$	$\beta \geq 0.234$	$\beta \geq 0.385$	$\beta \geq 0.510$	$\beta \geq 0.619$
$d_l = 7$	$\beta \geq 0.161$	$\beta \geq 0.282$	$\beta \geq 0.389$	$\beta \geq 0.487$
$d_l = 9$	$\beta \geq 0.134$	$\beta \geq 0.242$	$\beta \geq 0.341$	$\beta \geq 0.434$

TABLE I
EVALUATING THE MINIMUM β REQUIRED IN (44) FOR DIFFERENT PAIRS OF α, d_l.

The proposition shows that a 'high-quality' expander graph can be obtained with a random construction from a *bounded* degree sequence. The left node set, A, corresponds to all the nodes in the network, while the right node set, B, corresponds to the number of perturbation such that $\beta N = |\mathcal{S}_i|$ (gene dynamics) or $\beta N = S$ (opinion dynamics). As Proposition 3 shows that the parameter α controls the maximum recoverable sparsity of $\boldsymbol{a}_i^{\mathrm{row}}$, the second inequality in (44) gives the condition on the required value for β under different condition for α. Concretely, Table I gives the value for pairs of α, β satisfying (44) for different d_l. If α decreases, β decreases nearly proportionally. If d increases, β decreases towards α.

C. Step 3: Concluding the Proofs

Proof of Theorem 1. Define the scalar constant as $\alpha = \frac{2d}{N}$, where d is the degree of a node in the regular network. Applying Proposition 4 and using the assumptions in the Theorem show that the bi-graph $G(\mathcal{S}_i, V)$ is an $(d-1, d, \alpha, 1-1/(d-1))$-expander graph in high probability if the tuple of $\beta = \frac{|\mathcal{S}_i|}{N}$ and α satisfy the condition in (44). In particular, since

$$\beta = \frac{|\mathcal{S}_i|}{N} \approx \frac{K}{N} = \frac{\Omega(d)}{N}, \tag{45}$$

the condition (44) is satisfied.

Consequently, as the support of $\boldsymbol{E}_i$ in our case is given by $G(\mathcal{S}_i, V)$, Proposition 3 shows that the norm $\|\boldsymbol{E}_i\boldsymbol{x}\|_1$ is lower bounded by $\upsilon^\star\|\boldsymbol{x}\|_1$ if $\|\boldsymbol{x}\|_0 \leq \alpha N$ and

$$\upsilon^\star = e_{\min}\, d - 2(e_{\max} - e_{\min}) > 0. \tag{46}$$

Finally, observe that any optimal solution to (27) must satisfies $\|\hat{\boldsymbol{a}}_i^{\text{row}}\|_0 \leq \|\boldsymbol{a}_i^{\text{row}}\|_0$, therefore $\hat{\boldsymbol{a}}_i^{\text{row}} - \boldsymbol{a}_i^{\text{row}}$ is at most $2\|\boldsymbol{a}_i^{\text{row}}\|_0 \leq \alpha N$ sparse. Since the construction of $\boldsymbol{E}_i$ satisfies the requirement in Proposition 3, this implies

$$\begin{aligned} &\left\|\boldsymbol{E}_i\left(\hat{\boldsymbol{a}}_i^{\text{row}} - \boldsymbol{a}_i^{\text{row}}\right)\right\|_1 \geq \upsilon^\star \left\|\hat{\boldsymbol{a}}_i^{\text{row}} - \boldsymbol{a}_i^{\text{row}}\right\|_1 \\ &\quad\Longrightarrow \|\hat{\boldsymbol{a}}_i^{\text{row}} - \boldsymbol{a}_i^{\text{row}}\|_1 \leq (\upsilon^\star)^{-1} \left\|\boldsymbol{\Delta}_i^{\mathsf{gene}}\right\|_1. \end{aligned} \tag{47}$$

This completes the proof.

Proof of Theorem 2. Following from (40), we observe:

$$\begin{aligned} &\|\boldsymbol{B}^\top(\boldsymbol{I} - \text{Diag}(\boldsymbol{c})^{-1}\boldsymbol{A})^{-\top}\boldsymbol{x}\|_1 \\ &\geq \|\boldsymbol{B}^\top\boldsymbol{x}\|_1 - \|\boldsymbol{B}^\top\boldsymbol{A}^\top(\text{Diag}(\boldsymbol{c}) - \boldsymbol{A})^{-\top}\boldsymbol{x}\|_1, \end{aligned} \tag{48}$$

for all $\boldsymbol{x} \in \mathbb{R}^N$. Setting

$$\xi^\star := \frac{\|\boldsymbol{B}^\top\|_1\|\boldsymbol{A}^\top\|_1 \max_{i\in\{1,\ldots,N\}} \frac{1}{c_i}}{1 - \|\boldsymbol{A}^\top\text{Diag}(\boldsymbol{c})^{-1}\|_1}, \tag{49}$$

it can be shown that

$$\|\boldsymbol{B}^\top\boldsymbol{A}^\top(\text{Diag}(\boldsymbol{c}) - \boldsymbol{A})^{-\top}\boldsymbol{x}\|_1 \leq \xi^\star\|\boldsymbol{x}\|_1. \tag{50}$$

On the other hand, under the said condition on the network between stubborn and non-stubborn agents, if $\beta = S/N$ satisfies the condition in Proposition 4, then the support pattern of $\boldsymbol{B}^\top$ corresponds to an expander of parameter $(\ell, \ell, \alpha, 1-1/\ell)$ with high probability. From Table I, the maximum allowable α satisfies $\alpha \propto \beta$, we have $\alpha N = \Theta(d_{\max})$.

Consequently, by the optimality of $\hat{\boldsymbol{a}}_i^{\text{row}}$, the error vector $\hat{\boldsymbol{a}}_i^{\text{row}} - \boldsymbol{a}_i^{\text{row}}$ is at most $2\|\boldsymbol{a}_i^{\text{row}}\|_0$ sparse. Observe that we have $\alpha N = \Theta(d_{\max}) \geq 2\|\boldsymbol{a}_i^{\text{row}}\|_0$, invoking Proposition 3 with $\boldsymbol{\mathcal{E}} = \boldsymbol{B}^\top$ shows

$$\begin{aligned} &\|\Delta_i^{\mathsf{op}}\|_1 = \|\boldsymbol{B}^\top(\boldsymbol{I} - \text{Diag}(\boldsymbol{c})^{-1}\boldsymbol{A})^{-\top}(\hat{\boldsymbol{a}}_i^{\text{row}} - \boldsymbol{a}_i^{\text{row}})\|_1 \\ &\geq (\upsilon^\star - \xi^\star)\|\hat{\boldsymbol{a}}_i^{\text{row}} - \boldsymbol{a}_i^{\text{row}}\|_1. \end{aligned} \tag{51}$$

Observing that $\|\Delta_i^{\mathsf{op}}\|_1 = \mathcal{O}(\epsilon^{\mathsf{op}})$ concludes the proof.

V. Numerical Evaluation

This section presents numerical experiments for justifying our claims about the efficacy of network dynamics identification from stationary points. Precisely, we evaluate the proposed recovery procedure on synthetic data from complex systems with randomly generated networks and dynamics.

Before presenting the main results, it is important to note that the minimization for $\boldsymbol{a}$ in line 3 of Algorithm 1 can be decomposed into N *independent* sub-problems. To demonstrate the decomposition technique, we take the loss function used with dynamic perturbation as an example. Using the property of Kronecker products and the definition of $\boldsymbol{\mathcal{F}}\big(\overline{\boldsymbol{x}}^{(k)}, \overline{\boldsymbol{x}}^{(k)}; \boldsymbol{\theta}\big)$, the least square term reduces to

$$\begin{aligned} &\sum_{i=1}^N \left|b_i^{(k)} + \boldsymbol{1}_N^\top\big(\text{vec}(\boldsymbol{\mathcal{H}}^\top(\overline{\boldsymbol{x}}^{(k)}, \overline{\boldsymbol{x}}^{(k)}))_i \odot \boldsymbol{a}_i^{\text{row}}\big)\right|^2 \\ &:= \textstyle\sum_{i=1}^N \mathcal{L}_{k,i}(\boldsymbol{a}_i^{\text{row}}; \overline{\boldsymbol{x}}^{(k)}) \end{aligned} \tag{52}$$

such that $b_i^{(k)} := [\boldsymbol{g}(\overline{\boldsymbol{x}}^{(k)}) + \boldsymbol{u}^{(k)}(\infty)]_i$, $\text{vec}(\boldsymbol{\mathcal{H}}^\top(\overline{\boldsymbol{x}}^{(k)}, \overline{\boldsymbol{x}}^{(k)}))_i$ is the ith block of the N^2 dimensional vector $\text{vec}(\boldsymbol{\mathcal{H}}^\top(\overline{\boldsymbol{x}}^{(k)}, \overline{\boldsymbol{x}}^{(k)}))$ and $\boldsymbol{a}_i^{\text{row}}$ is the ith row vector of $\boldsymbol{A}$. Using this observation, we can express the sub-problem needed by line 3 of Algorithm 1 as:

$$\min_{\tilde{\boldsymbol{a}}_i^{\text{row}} \in \mathbb{R}_+^N, i=1,\ldots,N} \sum_{i=1}^N \Big(\frac{1}{K}\sum_{k=1}^K \mathcal{L}_{k,i}(\tilde{\boldsymbol{a}}_i^{\text{row}}; \overline{\boldsymbol{x}}^{(k)}) + \rho g_i(\tilde{\boldsymbol{a}}_i^{\text{row}})\Big), \tag{53}$$

which represents N *independent* sub-problems, each involving an N-dimensional vector. These problems can then be solved in a *parallel* fashion, each of the sub-problems can be solved with a worst case complexity of $\mathcal{O}(N^{3.5}\log(1/\epsilon))$, where $\epsilon > 0$ is the desired accuracy [44]. As we observe from the numerical experiments below, the proposed method can easily scale to large networks with $N \approx 1000$ nodes.

We test the performance of the proposed network dynamics identification method using randomly generated complex systems. Particularly, we consider three common types of random topology models [45] — Erdos-Renyi (ER), Watts-Strogatz (WS), and Preferential Attachment (PA), which are parameterized by the connect probability p_{ER}, the rewiring probability p_{WS} and minimum node degree d_{PA}, respectively. In some examples, we also test the method on random regular graphs with fixed degree for all nodes. Though the proposed method identifies directed graph, the graphs generated in the experiments are undirected. The network weights $\boldsymbol{A}$ are generated uniformly such that $A_{ij} = 1/d_i$ if $(j,i) \in E$ where d_i is the in-degree of node i. The stationary points (including the perturbed ones) are then generated as: 1) for gene dynamics, using the 4th order Runge-Kutte method [46]; 2) for opinion dynamics, through directly simulating the discretized version of (2) for $t = 500$ time steps using a random initialization of $x_i(0) \sim \mathcal{U}[-1, 1]$. For benchmarks, we focus on comparing the area under ROC (AUROC), area under precision-recall (AUPR), and normalized mean squared error (NMSE), defined as $\mathsf{NMSE} := \|\boldsymbol{A} - \hat{\boldsymbol{A}}\|_F^2/\|\boldsymbol{A}\|_F^2$ under different scenarios.

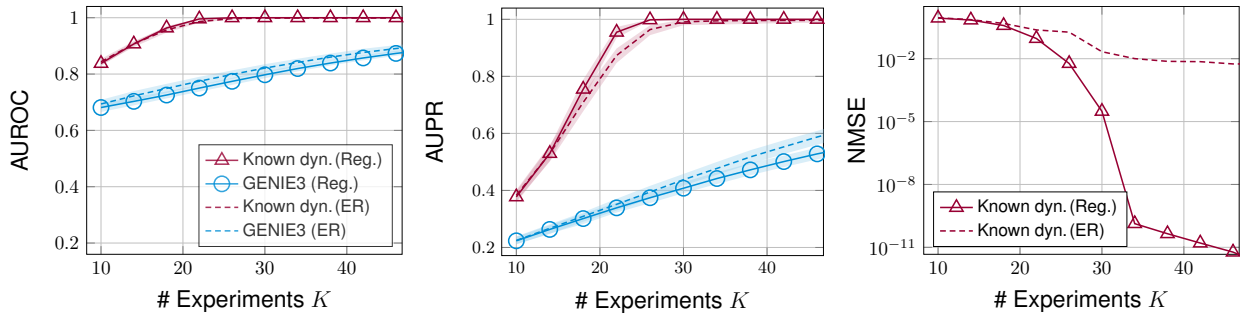

Fig. 2. **Inference Performance (unknown $\boldsymbol{a}$ and known $\boldsymbol{\theta}$) with gene dynamics and $N = 100$ nodes**. In the legend, 'ER' and 'Reg' refer to the experiments with ER and regular graphs, respectively. (Left) AUROC. (Middle) AUPR. (Right) NMSE. The shaded area denotes the 10th/90th percentile confidence interval.

A. Gene Dynamics and Topology Perturbations

As our first example we consider a small network ($N = 100$), driven by (7), in which we take (δ_i, γ_i) to be $(1, 0.5)$, and focus on inferring the network parameter $\boldsymbol{a} = (A_{ij})_{i=1,\dots,N, j=1,\dots N}$. We set the regularization parameter in (22) to $\rho = 10^{-8}$, noting that the performance is insensitive to the specific choice of ρ, and use the prior support set $\mathcal{S}$ in (20) with $\eta = 0.02$. Fig. 2 (a) and (b) show the performance comparison with ER graphs of $p_{\mathsf{ER}} = 2\log N/N$ and regular graphs with fixed degree at $d_{\mathsf{reg}} = 10$, note we have $p_{\mathsf{ER}} \approx d_{\mathsf{reg}}/N$. Moreover, the figures indicate that we achieve a perfect reconstruction, *i.e.,* AUROC, AUPR $\to 1$ already at $K \approx 25$ (red), namely that we achieve a complete reconstruction of A_{ij}'s $N^2 \sim 10^4$ unknown parameters with just 25 experiments. For comparison, GENIE3, the leading inference method in DREAM5 [13] achieves significantly lower scores, even as K approaches 50. In each simulated experiment, we remove a distinct randomly selected node $\pi(k) \in [N]$, and examine the dynamics response, extracting the final perturbed steady state from (7). We then use our method to infer $\boldsymbol{a}$, measuring the quality of our inference via AUROC and AUPR, representing standard tests for network inference assessment. Hence, our proposed method significantly outperformed GENIE3, whose performance strongly depends on the amount of stationary point data. The NMSE comparison shows that the network weights with regular graph are perfectly recovered when $K \geq 32$ (Fig. 2 (c)).

Next, we consider also unknown dynamics, seeking also to retrieve the value of $\boldsymbol{\theta}$. The same setting was used for simulating the stationary points as in the previous example. For this example, we apply grid search for $\boldsymbol{\theta}$ in the AO procedure over a grid with $\gamma, \delta \in \{0.1, 0.2, ..., 1\}$. We observe in Fig. 3 a similar trend, in which our method (red) achieves a higher score under lower K compared to GENIE3. This time, as $\boldsymbol{\theta}$ is also unknown, slightly more experiments are required to achieve perfect reconstruction ($K \approx 30$).

In Table II we simulate the performance on large-scale networks (with $N = 1000$) under known dynamics parameter $\boldsymbol{\theta}$. We examined ER graphs with $p_{\mathsf{ER}} = 1.1\log N/N$, WS graphs with average degree of $\log N$ and rewiring probability of $p_{\mathsf{WS}} = 0.2$, and PA graphs, a most empirically relevant structure [47], with minimum node degree of $d_{\mathsf{PA}} = 4$, such that the average degrees of these graphs are comparable. We observe that the number of experiments required K ($K \approx 150$ returns a reasonable performance for all cases) can be maintained at a small fraction of N. Interestingly, for gene regulation, we observe the best performance on the PA graphs. As such graphs are highly prevalent, we find this to be an encouraging result. The most challenging one is the WS graphs. This can be explained as a consequence of its unique structure, in which the sub-graphs formed by the out-going edges of the perturbed nodes do not correspond to a random regular bi-partite graph. This is a crucial condition required by the identifiability analysis in Section IV.

B. Opinion Dynamics with Dynamic Perturbations

We now consider perturbations on opinion dynamics introduced by stubborn agent as described in Fact 1. We examine the scenario with a *mismatched dynamics* model that the steady-state opinions are simulated using the bounded confidence model [cf. $\mu_b(\cdot)$ in Example 2] with threshold set to $\tau = 0.4$ for half of the agents, and $\tau = 0.6$ for the other half; the initial opinions are set to $x_i(0) \sim \mathcal{U}[-1, 1]$; meanwhile the dynamics inference is performed using a sigmoid approximation [cf. $\mu_c(\cdot)$ in Example 2] with $\sigma = 10$ and τ is an unknown parameter. For problem (22), we set $\rho = 10$. Moreover, the network from stubborn agents to non-stubborn agents [cf. $\boldsymbol{B}$ in (16)] is generated as a random regular bi-partite graph with degree 5.

Similar to the previous set of experiments on gene dynamics, we consider a small network ($N = 100$) example, and compare the inference performance against the number of stubborn agents S on two types of graphs: ER and WS graphs with $p_{\mathsf{ER}} = 2\log N/N$ and $p_{\mathsf{WS}} = 0.2$. Similar to the examples in gene dynamics, the expected degrees for the nodes are constant for the two network models. The inference is performed through observing $K = S$ steady state opinions. From Fig. 4, we observe that even under the non-ideal scenario with mismatched dynamics, the proposed method recovers the network accurately with improvement over GLASSO[3].

In Table II, we simulate the performance on large networks (with $N = 1000$) where the settings for random topologies are the same as in the gene dynamics of the same table. Again, we observe that the number of experiments required K can be maintained at a smaller fraction of N through exploiting sparsity in the network. In contrast to the gene dynamics case, we recall from Section IV that the identifiability condition depends on the network given by $\boldsymbol{B}$ which is constructed as a random regular bi-partite graph. The performance difference

[3]Code from: http://publish.illinois.edu/xiaohuichen/code/graphical-lasso/

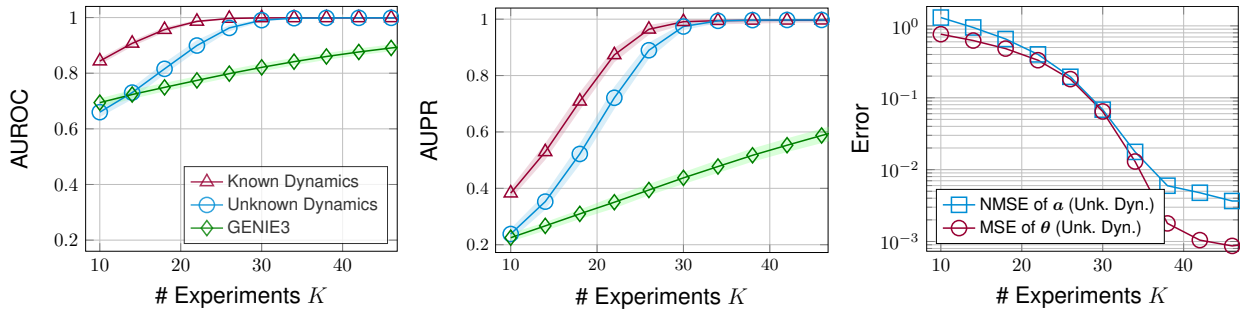

Fig. 3. **Inference Performance (unknown a and θ) with gene dynamics and $N = 100$ nodes**. (Left) AUROC. (Middle) AUPR. (Right) Error of estimating a and θ.

	Gene Dynamics			*Opinion Dynamics*		
Topology	$K = 100$	$K = 150$	$K = 200$	$K = 100$	$K = 150$	$K = 200$
ER	0.972/0.481	0.973/0.819	0.995/0.980	0.964/0.927	0.999/0.999	1.000/1.000
WS	0.971/0.752	0.971/0.870	0.962/0.923	0.999/0.999	1.000/1.000	1.000/1.000
PA	0.997/0.889	0.999/0.974	1.000/0.990	0.904/0.748	0.956/0.889	0.976/0.941

TABLE II

INFERENCE PERFORMANCE ON GENE, OPINION DYNAMICS (WITH UNKNOWN a AND KNOWN θ) WITH $N = 1000$ NODES. THE RESULTS SHOWN ARE AVERAGED OVER 10 REALIZATIONS, SHOWN IN THE ORDER OF 'AUROC/AUPR'.

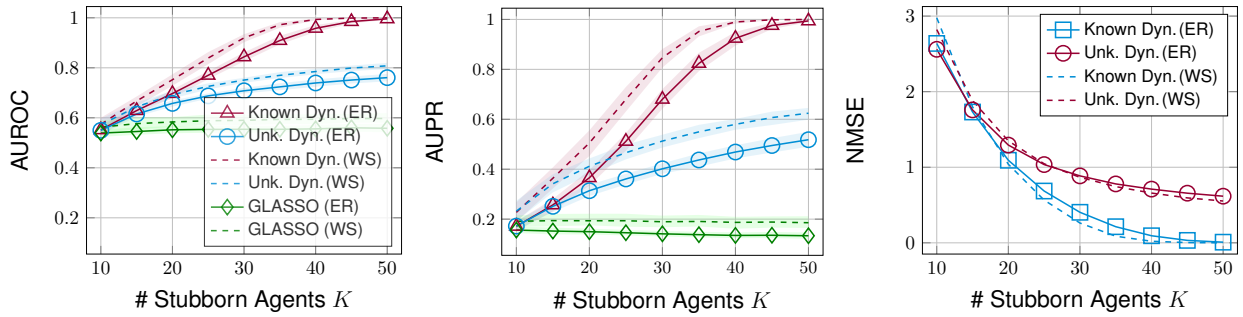

Fig. 4. **Inference Performance (unknown a and θ) with opinion dynamics and $N = 100$ nodes**. (Left) AUROC. (Middle) AUPR. (Right) NMSE. Shaded area is the 10th/90th percentile confidence interval.

between ER, WS and PA graphs rest solely on the variance of the degree distribution. As such, the proposed method performs best on WS graphs and worst on PA graphs.

The numerical analysis demonstrates that incorporating knowledge from physical model can lead to significant improvement in the inference accuracy. This further supports our claims on the identifiability of nonlinear dynamic systems.

VI. Empirical Data from Gene Regulatory Networks

The ultimate goal of our methodology is to reconstruct the complex system (2) from empirical data. Hence we collected data from real perturbation experiment on E. coli and S. cerevisiae, and used our framework to retrieve their hidden dynamics parameters. Lacking a ground truth for the dynamic parameters $\boldsymbol{a}, \boldsymbol{\theta}$, we test our method's performance against the common gold-standard for the *networks*, assuming that a high quality reconstruction of $\boldsymbol{a}$ is, in and of itself, indicative of a successful approximation of the dynamics.

a) DREAM5 Dataset: We test our method against the DREAM5 network inference challenge [13], which is an accepted benchmark for network inference methods. Focusing on *E. coli* and *S. cerevisiae*, we extracted a total of $K_T = 326$ (*E. Coli*) and $K_T = 238$ (*S. cerevisiae*) vectors of stationary points, each of $\boldsymbol{x}_\ell$, $\ell \in \{1, ..., K_T\}$ is a result of a perturbation experiment. Accounting for the data of repeated perturbation experiments of the same condition, the dataset includes $K = 56$ (*E. coli*), $K = 7$ (*S. cerevisiae*) distinct topology perturbation conditions. The target network consists of $N = 4,511$ (*E. coli*) and $N = 5,950$ (*S. cerevisiae*) genes. The dataset also features a set of $TF = 334$ (*E. coli*), $TF = 333$ (*S. cerevisiae*) transcription factors, which are the regulating genes, *i.e.,* genes with outgoing links; however, some percentage of marked transcription factors are wrongly labeled decoys.

b) Preprocessing Step: A key advantage of network inference from stationary points is that one could aggregate noisy observations from repeated experiments. To exploit that, for the DREAM5 dataset, we partition the dataset of stationary points as $[K_T] = \mathcal{K}_0 \cup \mathcal{K}_1 \cup \cdots \cup \mathcal{K}_K$ such that $\mathcal{K}_0$ is the set of stationary points under no perturbation, and $\mathcal{K}_k \subseteq [K_T]$ corresponds to the kth topology perturbation. Assuming that the complex system (2) has a unique stationary point, we can write

$$\begin{aligned} &\boldsymbol{x}_\ell = \overline{\boldsymbol{x}}^{(0)} + \boldsymbol{w}_\ell, \ \forall\ \ell \in \mathcal{K}_0 \\ &\implies \boldsymbol{X}^{(0)} := (\boldsymbol{x}_\ell)_{\ell \in \mathcal{K}_0} = \overline{\boldsymbol{x}}^{(0)} \mathbf{1}^\top + \boldsymbol{W}_0, \end{aligned} \tag{54}$$

	E. coli			*S. cerevisiae*		
Methods	AUROC	AUPR	Score	AUROC	AUPR	Score
TIGRESS [48]	0.595	0.069	4.41	0.517	0.02	1.082
GENIE3 [6]	0.617	**0.093**	14.79	0.518	0.021	1.387
RankSum [13]	0.65	0.09	24.90	**0.528**	**0.022**	**6.236**
Proposed (*top* 10^5)	**0.6823** 3.13×10^{-66}	0.0508 8.5×10^{-2}	**33.29**	0.525 6.47×10^{-8}	0.021 2.9×10^{-2}	4.161
GENIMS [8]	0.705	0.052	48.33	0.533	0.02	8.454
Proposed (*top* 5×10^5)	**0.7573** 1.04×10^{-184}	**0.0574** 2.7×10^{-3}	**93.28**	**0.5734** 1.5×10^{-119}	**0.0252** 2.38×10^{-7}	**62.64**

*All scores are calculated from the top 10^5 predictions. Exceptions are GENIMS and proposed method (top 5×10^5) that are based on all, and top 5×10^5 predictions, respectively.

TABLE III

INFERENCE PERFORMANCE ON TWO EMPIRICAL DATASET. THE LOWER COLUMNS' SCORES ARE THE p-VALUES FOR THE AUROC/AUPR METRICS. MOREOVER, THE PROPOSED METHOD FINDS THE PARAMETERS AS $\delta = 0.047, \gamma = 0.5893$ FOR *E. coli* AND $\delta = 0.5571, \gamma = 0.3749$ FOR *S. cerevisiae*.

where we stacked up the stationary points in $\mathcal{K}_0$ to form the matrix $\boldsymbol{X}^{(0)} := (\boldsymbol{x}_\ell)_{\ell \in \mathcal{K}_0} \in \mathbb{R}^{N \times |\mathcal{K}_0|}$, and $\boldsymbol{w}_\ell$ models the variation due to imperfection in the experiments. When the noise is small, $\boldsymbol{X}^{(0)}$ is close to rank-one. Therefore, defining $\boldsymbol{u}_1^{(0)}$ as the top left eigenvector of $\boldsymbol{X}^{(0)}$ and σ_1 as its associated eigenvalue, we can estimate $\overline{\boldsymbol{x}}^{(0)}$ by

$$\widehat{\boldsymbol{x}}^{(0)} = \sigma_1 \, \boldsymbol{u}_1^{(0)}. \tag{55}$$

We then denote by $\boldsymbol{U}_{-1}^{(0)}$ the remaining eigenvectors of $\boldsymbol{X}^{(0)}$ and use the fact that $\widehat{\boldsymbol{x}}^{(0)}$ is in the null space of $\boldsymbol{U}_{-1}^{(0)}$, to estimate $\overline{\boldsymbol{x}}^{(k)}$ by

$$\widehat{\boldsymbol{x}}^{(k)} = \widehat{\boldsymbol{x}}^{(0)} + \tfrac{1}{|\mathcal{K}_k|} \boldsymbol{U}_{-1}^{(0)} (\boldsymbol{U}_{-1}^{(0)})^\top \textstyle\sum_{\ell \in \mathcal{K}_k} \boldsymbol{x}_\ell, \tag{56}$$

where the second term on the right hand side is an estimate of $\overline{\boldsymbol{x}}^{(k)} - \overline{\boldsymbol{x}}^{(0)}$. Often we have $|\mathcal{K}_0| \gg |\mathcal{K}_k|$ with DREAM5 being no exception, having $|\mathcal{K}_0| = 139$, $|\mathcal{K}_k| \approx 5$ for each $k \geq 1$ (*E. coli*) and $|\mathcal{K}_0| = 107$, $|\mathcal{K}_k| \approx 4$ for each $k \geq 1$ (*S.cerevisiae*). Hence, the unperturbed stationary points can, in principle, be estimated with high reliability, providing firm grounds for the inference. For the perturbed stationary points, since $|\mathcal{K}_k|$ is small, we observe that a simple aggregation procedure suffices as $\widehat{\boldsymbol{x}}^{(k)} - \widehat{\boldsymbol{x}}^{(0)}$ is orthogonal to $\widehat{\boldsymbol{x}}^{(0)}$.

c) Parameters: We set $\eta = 0.005$ for the support set estimator [$\mathcal{S}_\eta$ in (20)]. In (22), The regularization parameters (ρ, γ, ζ) are set to $(3, 1, \frac{5}{3})$ (*resp.* $(3 \times 10^{-1}, 1, \frac{5}{3})$) for the *E. coli* (*resp. S. cerevisiae*) network. The AO procedure tackles (22) with the function template (7) and a projected gradient (PG) step on $\boldsymbol{\theta}$, which has several parameters to be initialized — for each $i \in [N]$, we initialize by setting $(\gamma_i, \delta_i) = (0.5, 0.5)$ and the step size of PG is set to 1×10^{-2}. Lastly, the AO procedure is set to terminate after 10 iterations.

d) Results: In the DREAM5 framework one ranks all links according to their inferred confidence levels. Then, using the top 10^5 links, the inference is confronted with the DREAM5 gold-standard in terms of AUROC and AUPR, assigning to each a p-value, p_{AUROC} and p_{AUPR}. The method score is then calculated via $\mathsf{Score} := \frac{\log_{10} p_{\mathsf{AUROC}} + \log_{10} p_{\mathsf{AUPR}}}{2}$. The results presented in Table III indicate that our proposed method achieves the highest score for *E. coli*, and the second highest for *S. cerevisiae*, outperforming the top scoring inference methods in DREAM5. The comparison with GENIMS [8] includes the top 5×10^5 predictions, to be consistent with the GENIMS data, that used this number of links. Under these conditions we find our method achieves overwhelmingly high scores, topping all other contenders. Note that TIGRESS [48] is also a top performing method of the DREAM5 challenge and GENIMS is an improved method from GENIE3. These results demonstrate that our method is able to infer the GRN from *few steady-state data*, while improving the performance compared to the state-of-the-art. This is despite the fact that we limited ourselves to only use steady state data, hence ignoring the transient data, which was available to the competing methods. In particular, our top performance on *E. coli* was achieved with only $\sim 40\%$ of the data provided by DREAM5.

VII. CONCLUSIONS

In this paper, we studied the network dynamics identification problem for recovering a complex system from observations of its stationary points. The problem of interest encompasses a simultaneous recovery of network topology and dynamics parameters. We proposed an efficient numerical method and showed that the network topology is identifiable under the restriction that the observation encompasses only a *limited number* of stationary points, which is small relative to the network size. The latter feature is desirable as empirical dataset available are often rank deficient. We verify the efficacy of our method on both synthetic and empirical data.

ACKNOWLEDGEMENT

The authors wish to thank Profs. Alessandro Rizzo and Guido Calderelli for insightful comments. The work of HTW, AS, AL was supported by National Science Foundation CCF-BSF 1714672. The work of BB was supported by a grant from the Ministry of Science & Technology, Israel & Ministry of foreign Affairs and international cooperation general directorate for country promotion, Italian Republic.

APPENDIX A
PROOF OF LEMMA 1

Consider the stationary point condition for the kth perturbation. For all $i \in [N]$, we have

$$\begin{aligned} 0 = &\textstyle\sum_{j=1}^N A_{ij} \mu(|\overline{x}_j^{(k)} - \overline{x}_i^{(k)}|)\big(\overline{x}_j^{(k)} - \overline{x}_i^{(k)}\big) \\ &+ \textstyle\sum_{j=1}^S B_{ij} \mu(|z_j^{(k)} - \overline{x}_i^{(k)}|)\big(z_j^{(k)} - \overline{x}_i^{(k)}\big) \end{aligned} \tag{57}$$

The lemma is proven from the definition of $\tilde{\boldsymbol{A}}^{(k)}$, $\tilde{\boldsymbol{B}}^{(k)}$ and stacking up the N equations above.

Appendix B
Proof of Proposition 1

Without loss of generality, we consider $\pi(k) = k$ such that the kth perturbation removes the kth node. Let us write

$$\overline{\boldsymbol{x}} - \overline{\boldsymbol{x}}^{(k)} = [\overline{\boldsymbol{x}}]_k \mathbf{e}_k + \boldsymbol{\epsilon} \;\text{ such that }\; [\boldsymbol{\epsilon}]_k = 0. \tag{58}$$

Our goal is to find $\boldsymbol{\epsilon}$ in the above. From the steady-state equation (12), observe

$$\overline{\boldsymbol{x}} - \overline{\boldsymbol{x}}^{(k)} = \boldsymbol{A}(\boldsymbol{h}(\overline{\boldsymbol{x}};\boldsymbol{\theta}) - \boldsymbol{h}(\overline{\boldsymbol{x}}^{(k)};\boldsymbol{\theta})) + \mathbf{e}_k\mathbf{e}_k^\top \boldsymbol{A}\boldsymbol{h}(\overline{\boldsymbol{x}}^{(k)};\boldsymbol{\theta}). \tag{59}$$

Notice that $\mathbf{e}_k$ is in the null space of $(\boldsymbol{I} - \mathbf{e}_k\mathbf{e}_k^\top)$. Therefore, combining (58) and (59) and left multiplying $(\boldsymbol{I} - \mathbf{e}_k\mathbf{e}_k^\top)$ to the both sides of the equations yields:

$$\begin{aligned}\boldsymbol{\epsilon} &= (\boldsymbol{I} - \mathbf{e}_k\mathbf{e}_k^\top)\boldsymbol{A}\big(\boldsymbol{h}(\overline{\boldsymbol{x}};\boldsymbol{\theta}) - \boldsymbol{h}(\overline{\boldsymbol{x}}^{(k)};\boldsymbol{\theta})\big)\\ &\overset{(a)}{\approx} (\boldsymbol{I} - \mathbf{e}_k\mathbf{e}_k^\top)\boldsymbol{A}\nabla\boldsymbol{h}(\overline{\boldsymbol{x}}^{(k)};\boldsymbol{\theta})([\overline{\boldsymbol{x}}]_k\mathbf{e}_k + \boldsymbol{\epsilon})\end{aligned} \tag{60}$$

where (a) is obtained by the Taylor's approximation for $\boldsymbol{h}(\overline{\boldsymbol{x}})$ centered at $\overline{\boldsymbol{x}}^{(k)}$. Expanding terms inside the bracket implies

$$\begin{aligned}\boldsymbol{\epsilon} \approx\; &(\boldsymbol{I} - \mathbf{e}_k\mathbf{e}_k^\top)\boldsymbol{A}\nabla\boldsymbol{h}(\overline{\boldsymbol{x}}^{(k)};\boldsymbol{\theta})\,\boldsymbol{\epsilon}\\ &+ [\overline{\boldsymbol{x}}]_k(\boldsymbol{I} - \mathbf{e}_k\mathbf{e}_k^\top)\boldsymbol{A}\nabla\boldsymbol{h}(\overline{\boldsymbol{x}}^{(k)};\boldsymbol{\theta})\mathbf{e}_k\end{aligned} \tag{61}$$

We notice that $\nabla\boldsymbol{h}(\overline{\boldsymbol{x}}^{(k)};\boldsymbol{\theta})$ is a diagonal matrix with $\frac{\partial h(x;\boldsymbol{\theta})}{\partial x}|_{x=\overline{x}_i^{(k)}}$ on its (i,i)th entry and $\overline{x}_k^{(k)} = 0$, therefore the latter term can be simplified as

$$\begin{aligned}&[\overline{\boldsymbol{x}}]_k(\boldsymbol{I} - \mathbf{e}_k\mathbf{e}_k^\top)\boldsymbol{A}\nabla\boldsymbol{h}(\overline{\boldsymbol{x}}^{(k)};\boldsymbol{\theta})\mathbf{e}_k\\ &= [\overline{\boldsymbol{x}}]_k \tfrac{\partial h(x;\boldsymbol{\theta})}{\partial x}|_{x=0}(\boldsymbol{I} - \mathbf{e}_k\mathbf{e}_k^\top)\boldsymbol{a}_k^{\text{col}}\\ &= [\overline{\boldsymbol{x}}]_k \tfrac{\partial h(x;\boldsymbol{\theta})}{\partial x}|_{x=0}\boldsymbol{a}_k^{\text{col}},\end{aligned} \tag{62}$$

where the last equality is due to the fact that the kth element of $\boldsymbol{a}_k^{\text{col}}$ is zero. We thus have

$$\boldsymbol{\epsilon} \approx (\boldsymbol{I} - \mathbf{e}_k\mathbf{e}_k^\top)\boldsymbol{A}\nabla\boldsymbol{h}(\overline{\boldsymbol{x}}^{(k)};\boldsymbol{\theta})\,\boldsymbol{\epsilon} + [\overline{\boldsymbol{x}}]_k \tfrac{\partial h(x;\boldsymbol{\theta})}{\partial x}|_{x=0}\,\boldsymbol{a}_k^{\text{col}}. \tag{63}$$

Observe that (63) is recursive in $\boldsymbol{\epsilon}$, therefore if we denote $\tilde{x} := [\overline{\boldsymbol{x}}]_k \frac{\partial h(x;\boldsymbol{\theta})}{\partial x}|_{x=0}$, then

$$\begin{aligned}\boldsymbol{\epsilon} &= \tilde{x}\big(\boldsymbol{I} - (\boldsymbol{I} - \mathbf{e}_k\mathbf{e}_k^\top)\boldsymbol{A}\nabla\boldsymbol{h}(\overline{\boldsymbol{x}}^{(k)};\boldsymbol{\theta})\big)^{-1}\boldsymbol{a}_k^{\text{col}}\\ &= \tilde{x}\Big(\boldsymbol{I} + (\boldsymbol{I} - \mathbf{e}_k\mathbf{e}_k^\top)\boldsymbol{A}\nabla\boldsymbol{h}(\overline{\boldsymbol{x}}^{(k)};\boldsymbol{\theta}) +\\ &\qquad ((\boldsymbol{I} - \mathbf{e}_k\mathbf{e}_k^\top)\boldsymbol{A}\nabla\boldsymbol{h}(\overline{\boldsymbol{x}}^{(k)};\boldsymbol{\theta}))^2 + \cdots\Big)\boldsymbol{a}_k^{\text{col}}\\ &\approx \tilde{x}\,\boldsymbol{a}_k^{\text{col}} = [\overline{\boldsymbol{x}}]_k \tfrac{\partial h(x;\boldsymbol{\theta})}{\partial x}|_{x=0}\,\boldsymbol{a}_k^{\text{col}},\end{aligned} \tag{64}$$

where the second equality is due to the Taylor's expansion. Notice that the series expansion holds when $\lambda_{max}((\boldsymbol{I} - \mathbf{e}_k\mathbf{e}_k^\top)\boldsymbol{A}\nabla\boldsymbol{h}(\overline{\boldsymbol{x}}^{(k)};\boldsymbol{\theta})) < 1$.

Appendix C
Proof of Lemma 2

The proof follows from the classical theory for compressed sensing, e.g., [42]. Without loss of generality, consider dynamics perturbation and observe that (18) solves the compressive sensing problem that can be simplified as:

$$\min_{\hat{\boldsymbol{a}}} \;\|\hat{\boldsymbol{a}}\|_0 \;\text{ s.t. }\; \boldsymbol{S}\boldsymbol{a} = \boldsymbol{S}\hat{\boldsymbol{a}}, \;\; [\hat{\boldsymbol{a}}]_{\mathcal{S}} = \mathbf{0}. \tag{65}$$

Clearly, $\hat{\boldsymbol{a}} = \boldsymbol{a}$ is a feasible solution to the problem above. Moreover, suppose that there exists a feasible $\tilde{\boldsymbol{a}}$ with $\|\tilde{\boldsymbol{a}}\|_0 \le \|\boldsymbol{a}\|_0 \le K$, we obtain that:

$$\mathbf{0} = \boldsymbol{S}(\boldsymbol{a} - \tilde{\boldsymbol{a}}) = [\boldsymbol{S}]_{:,\text{supp}(\boldsymbol{a}-\tilde{\boldsymbol{a}})}\boldsymbol{x}, \tag{66}$$

where $\boldsymbol{x} = [\boldsymbol{a} - \tilde{\boldsymbol{a}}]_{\text{supp}(\boldsymbol{a}-\tilde{\boldsymbol{a}})}$ and $\text{supp}(\boldsymbol{a})$ is the set of non-zeros for a vector $\boldsymbol{a}$. Since $\text{spark}(\boldsymbol{A}) \ge 2K + 1 \ge |\text{supp}(\boldsymbol{a} - \tilde{\boldsymbol{a}})|$, the sub-matrix $[\boldsymbol{S}]_{:,\text{supp}(\boldsymbol{a}-\tilde{\boldsymbol{a}})}$ is full-rank. This implies that $\boldsymbol{x} = \mathbf{0}$ and thus $\boldsymbol{a} = \tilde{\boldsymbol{a}}$. The proof is concluded.

Appendix D
Proof of Proposition 3

Our proof follows a similar line of arguments as in [27, Proposition 3]. Let $\boldsymbol{x} \in \mathbb{R}^N$ be an $2s$-sparse vector with its support set denoted as $\text{supp}(\boldsymbol{x}) := \{i \in [N] : x_i \neq 0\}$. The definition of expander graphs implies

$$\delta d_l\,|S| \le \delta\,|E(S,B)| \le |N(S)|, \tag{67}$$

for all $S \subseteq \text{supp}(\boldsymbol{x}) \subseteq A$ since $|\text{supp}(\boldsymbol{x})| \le 2s \le \alpha N$. The Hall's theorem [49] shows that there are δd_l disjoint matchings for $\text{supp}(\boldsymbol{x})$, a subset of the left node set A. We decompose $\boldsymbol{E}_i$ as:

$$\boldsymbol{E}_i = \boldsymbol{E}_M + \boldsymbol{E}_C, \tag{68}$$

such that $\text{supp}(\boldsymbol{E}_M) \cap \text{supp}(\boldsymbol{E}_C) = \emptyset$. Moreover, $\text{supp}(\boldsymbol{E}_M)$ corresponds to the δd_l disjoint matchings for $\text{supp}(\boldsymbol{x})$ such that each row of $\boldsymbol{E}_M$ has at most one non-zero entry and each column has exactly δd_l non-zero entries; and the remainder $\boldsymbol{E}_C$ has at most $d_u - \delta d_l$ non-zero entries per column. Notice that this implies $\|\boldsymbol{E}_M\boldsymbol{x}\|_1 \ge e_i^{\min}\,\delta d_l\,\|\boldsymbol{x}\|_1$ and $\|\boldsymbol{E}_C\boldsymbol{x}\|_1 \le e_i^{\max}\,(d_u - \delta d_l)\,\|\boldsymbol{x}\|_1$. Therefore,

$$\begin{aligned}\|\boldsymbol{E}_i\boldsymbol{x}\|_1 &= \|(\boldsymbol{E}_M + \boldsymbol{E}_C)\boldsymbol{x}\|_1\\ &\ge \big(e_i^{\min}\,\delta d_l - e_i^{\max}\,(d_u - \delta d_l)\big)\|\boldsymbol{x}\|_1.\end{aligned} \tag{69}$$

This concludes the proof of the proposition.

References

[1] H.-T. Wai, A. Scaglione, B. Barzel, and A. Leshem, "Network inference from complex systems steady states: Theory and methods," in *Proc DSW*, April 2018.

[2] T. Ideker and R. Sharan, "Protein networks in disease," *Genome research*, vol. 18, no. 4, pp. 644–652, 2008.

[3] M. Buchanan, G. Caldarelli, P. De Los Rios, F. Rao, and M. Vendruscolo, *Networks in cell biology*. Cambridge University Press, 2010.

[4] B. Barzel, Y.-Y. Liu, and A.-L. Barabási, "Constructing minimal models for complex system dynamics," *Nature communications*, vol. 6, p. 7186, 2015.

[5] R. Küffner, T. Petri, P. Tavakkolkhah, L. Windhager, and R. Zimmer, "Inferring gene regulatory networks by anova," *Bioinformatics*, vol. 28, no. 10, pp. 1376–1382, 2012.

[6] V. Huynh-Thu, A. Irrthum, L. Wehenkel, and P. Geurts, "Inferring regulatory networks from expression data using tree-based methods," *PLoS ONE*, vol. 5, no. 9, 2010.

[7] F. Petralia, P. Wang, J. Yang, and Z. Tu, "Integrative random forest for gene regulatory network inference," *Bioinformatics*, vol. 31, no. 12, pp. i197–i205, 2015.

[8] J. Wu, X. Zhao, Z. Lin, and Z. Shao, "Large scale gene regulatory network inference with a multi-level strategy," *Molecular bioSystems*, vol. 12, no. 2, pp. 588–597, 2016.

[9] J. Friedman, T. Hastie, and R. Tibshirani, "Sparse inverse covariance estimation with the graphical lasso," *Biostatistics*, vol. 9, no. 3, pp. 432–441, 2008.

[10] M. Drton and M. H. Maathuis, "Structure learning in graphical modeling," *Annual Review of Statistics and Its Application*, vol. 4, pp. 365–393, 2017.

[11] A. J. Rothman, P. J. Bickel, E. Levina, J. Zhu *et al.*, "Sparse permutation invariant covariance estimation," *Electronic Journal of Statistics*, vol. 2, pp. 494–515, 2008.

[12] P. Ravikumar, M. J. Wainwright, G. Raskutti, and B. Yu, "High-dimensional covariance estimation by minimizing ℓ1-penalized log-determinant divergence," *Electronic Journal of Statistics*, vol. 5, pp. 935–980, 2011.

[13] D. Marbach, J. C. Costello, R. Küffner, N. M. Vega, R. J. Prill, D. M. Camacho, K. R. Allison, A. Aderhold, R. Bonneau, Y. Chen *et al.*, "Wisdom of crowds for robust gene network inference," *Nature methods*, vol. 9, no. 8, p. 796, 2012.

[14] M. Timme, "Revealing network connectivity from response dynamics," *Physical review letters*, vol. 98, no. 22, p. 224101, 2007.

[15] W.-X. Wang, Y.-C. Lai, C. Grebogi, and J. Ye, "Network Reconstruction Based on Evolutionary-Game Data via Compressive Sensing," *Physical Review X*, vol. 1, no. 2, pp. 1–7, 2011.

[16] D. Bertsimas, V. Gupta, and I. C. Paschalidis, "Data-driven estimation in equilibrium using inverse optimization," *Mathematical Programming*, vol. 153, no. 2, pp. 595–633, 2015.

[17] A. Chen, J. Cao, and T. Bu, "Network tomography: Identifiability and fourier domain estimation," *IEEE Transactions on Signal Processing*, vol. 58, no. 12, pp. 6029–6039, 2010.

[18] J. O. Ramsay, G. Hooker, D. Campbell, and J. Cao, "Parameter estimation for differential equations: a generalized smoothing approach," *Journal of the Royal Statistical Society: Series B (Statistical Methodology)*, vol. 69, no. 5, pp. 741–796, 2007.

[19] H. Miao, X. Xia, A. S. Perelson, and H. Wu, "On identifiability of nonlinear ode models and applications in viral dynamics," *SIAM review*, vol. 53, no. 1, pp. 3–39, 2011.

[20] H. E. Egilmez, E. Pavez, and A. Ortega, "Graph learning from data under laplacian and structural constraints," *IEEE Journal of Selected Topics in Signal Processing*, vol. 11, no. 6, pp. 825–841, 2017.

[21] S. Segarra, A. G. Marques, G. Mateos, and A. Ribeiro, "Network topology inference from spectral templates," *IEEE Transactions on Signal and Information Processing over Networks*, vol. 3, no. 3, pp. 467–483, 2017.

[22] S. P. Chepuri, S. Liu, G. Leus, and A. O. Hero, "Learning sparse graphs under smoothness prior," March 2017, pp. 6508–6512.

[23] X. Dong, D. Thanou, P. Frossard, and P. Vandergheynst, "Learning laplacian matrix in smooth graph signal representations," *IEEE Transactions on Signal Processing*, vol. 64, no. 23, pp. 6160–6173, 2016.

[24] V. Kalofolias, "How to learn a graph from smooth signals," in *Artificial Intelligence and Statistics*, 2016, pp. 920–929.

[25] J. Mei and J. M. Moura, "Signal processing on graphs: Causal modeling of unstructured data," *IEEE Transactions on Signal Processing*, vol. 65, no. 8, pp. 2077–2092, 2017.

[26] X. Cai, J. A. Bazerque, and G. B. Giannakis, "Inference of gene regulatory networks with sparse structural equation models exploiting genetic perturbations," *PLoS computational biology*, vol. 9, no. 5, p. e1003068, 2013.

[27] H.-T. Wai, A. Scaglione, and A. Leshem, "Active sensing of social networks," *IEEE Transactions on Signal and Information Processing over Networks*, vol. 2, no. 3, pp. 406–419, 2016.

[28] Y. Shen, B. Baingana, and G. B. Giannakis, "Kernel-based structural equation models for topology identification of directed networks," *IEEE Transactions on Signal Processing*, vol. 65, no. 10, pp. 2503–2516, 2017.

[29] V. N. Ioannidis, Y. Shen, and G. B. Giannakis, "Semi-blind inference of topologies and dynamical processes over graphs," *arXiv preprint arXiv:1805.06095*, 2018.

[30] C. Ravazzi, R. Tempo, and F. Dabbene, "Learning influence structure in sparse social networks," *IEEE Transactions on Control of Network Systems*, 2017.

[31] H.-T. Wai, S. Segarra, A. E. Ozdaglar, A. Scaglione, and A. Jadbabaie, "Blind community detection from low-rank excitations of a graph filter," *arXiv preprint arXiv:1809.01485*, 2018.

[32] H. K. Khalil, "Nonlinear systems," *Prentice-Hall, New Jersey*, vol. 2, no. 5, pp. 5–1, 1996.

[33] U. Alon, *An introduction to systems biology: design principles of biological circuits*. Chapman and Hall/CRC, 2006.

[34] G. Karlebach and R. Shamir, "Modelling and analysis of gene regulatory networks," *Nature Reviews Molecular Cell Biology*, vol. 9, no. 10, p. 770, 2008.

[35] M. H. DeGroot, "Reaching a consensus," *Journal of the American Statistical Association*, vol. 69, no. 345, pp. 118–121, 1974.

[36] R. Hegselmann, U. Krause *et al.*, "Opinion dynamics and bounded confidence models, analysis, and simulation," *Journal of artificial societies and social simulation*, vol. 5, no. 3, 2002.

[37] L. Li, A. Scaglione, A. Swami, and Q. Zhao, "Consensus, polarization and clustering of opinions in social networks," *IEEE Journal on Selected Areas in Communications*, vol. 31, no. 6, pp. 1072–1083, 2013.

[38] D. Acemoglu, A. Ozdaglar, and A. ParandehGheibi, "Spread of (mis) information in social networks," *Games and Economic Behavior*, vol. 70, no. 2, pp. 194–227, 2010.

[39] B. Barzel and A.-L. Barabási, "Universality in network dynamics," *Nature physics*, vol. 9, no. 10, p. 673, 2013.

[40] S. Maslov, K. Sneppen, and I. Ispolatov, "Spreading out of perturbations in reversible reaction networks," *New journal of physics*, vol. 9, no. 8, p. 273, 2007.

[41] M. Razaviyayn, M. Hong, and Z.-Q. Luo, "A unified convergence analysis of block successive minimization methods for nonsmooth optimization," *SIAM Journal on Optimization*, vol. 23, no. 2, pp. 1126–1153, 2013.

[42] S. Foucart and H. Rauhut, *A mathematical introduction to compressive sensing*. Birkhäuser Basel, 2013, vol. 1, no. 3.

[43] S. Hoory, N. Linial, and A. Wigderson, "Expander graphs and their applications," *Bulletin of the American Mathematical Society*, vol. 43, no. 4, pp. 439–561, 2006.

[44] A. Ben-Tal and A. Nemirovski, *Lectures on modern convex optimization: analysis, algorithms, and engineering applications*. Siam, 2001, vol. 2.

[45] M. E. Newman, "Networks: an introduction," 2011.

[46] J. C. Butcher, *Numerical methods for ordinary differential equations*. John Wiley & Sons, 2016.

[47] A.-L. Barabási and R. Albert, "Emergence of scaling in random networks," *science*, vol. 286, no. 5439, pp. 509–512, 1999.

[48] A.-C. Haury, F. Mordelet, P. Vera-Licona, and J.-P. Vert, "Tigress: trustful inference of gene regulation using stability selection," *BMC systems biology*, vol. 6, no. 1, p. 145, 2012.

[49] D. B. West, *Introduction to graph theory*. Prentice hall Upper Saddle River, 2001, vol. 2.

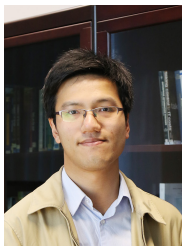

Hoi-To Wai (S'11–M'18) received his PhD degree from Arizona State University (ASU) in Electrical Engineering in Fall 2017, B. Eng. (with First Class Honor) and M. Phil. degrees in Electronic Engineering from The Chinese University of Hong Kong (CUHK) in 2010 and 2012, respectively. He is an Assistant Professor in the Department of Systems Engineering & Engineering Management at CUHK. He has held research positions at ASU, UC Davis, Telecom ParisTech, Ecole Polytechnique, LIDS, MIT.

Hoi-To's research interests are in the broad area of signal processing, machine learning and distributed optimization, with a focus of their applications to network science. His dissertation has received the 2017's Dean's Dissertation Award from the Ira A. Fulton Schools of Engineering of ASU and he is a recipient of a Best Student Paper Award at ICASSP 2018.

Anna Scaglione (M.Sc.'95, Ph.D. '99, F'11) is a professor in electrical and computer engineering at Arizona State University. She was Professor of Electrical Engineering previously at UC Davis (2010-2014), Associate Professor at UCD 2008-2010 and Cornell (2006-2008), and Assistant Professor at Cornell (2001-2006) and at the University of New Mexico (2000-2001). Her expertise is in statistical signal processing and here research focuses on its various applications in network and data science, including distributed protocols, information systems and intelligent infrastructure, particularly for energy delivery systems. Dr. Scaglione was elected an IEEE fellow in 2011. She is Distinguished Lecturer for the IEEE Signal Processing Society for 2019-2020. She received the 2000 IEEE Signal Processing Transactions Best Paper Award and more recently was honored for the 2013, IEEE Donald G. Fink Prize Paper Award for the best review paper in that year in the IEEE publications, her work with her student earned 2013 IEEE Signal Processing Society Young Author Best Paper Award.

Baruch Barzel is a physicist and applied mathematician, director of the Complex Network Dynamics lab at the Bar-Ilan University Mathematics department. His main research areas are statistical physics, complex systems, nonlinear dynamics and network science. His specific focus is on the dynamic behavior of complex networks, uncovering universal principles that govern the dynamics of diverse systems, such as disease spreading, gene regulatory networks, protein interactions or population dynamics. Barzel completed his Ph.D. in physics at the Hebrew University of Jerusalem, Israel as a Hoffman Fellow. He then pursued his postdoctoral training at the Center for Complex Network Research at Northeastern University and at the Channing Division of Network Medicine, Harvard Medical School. Dr. Barzel received the Racah prize for excellence in research in 2007 and the Krill Prize awarded by the Wolf Foundation in 2018.

Amir Leshem (SM'06) received his B.Sc. (Cum Laude) in mathematics and physics, his M.Sc. (Cum Laude) in mathematics, and his Ph.D. in mathematics all from the Hebrew University, Jerusalem, Israel, in 1986, 1990 and 1998 respectively. From 1998 to 2000 he was with Faculty of Information Technology and Systems, Delft University of Technology, The Netherlands, as a postdoctoral fellow working on algorithms for the reduction of terrestrial electromagnetic interference in radio-astronomical radio telescope antenna arrays and signal processing for communication. From 2000 to 2003 he was the director of advanced technologies at Metalink Broadband where he was responsible for research and development of new DSL and wireless MIMO modem technologies and served as a member of several international standard setting groups such as ITU-T SG15, ETSI TM06, NIPP-NAI, IEEE 802.3 and 802.11. From 2000 to 2002 he was also a visiting researcher at Delft University of Technology. In 2002 he joined Bar-Ilan University and was one of the founders of the Faculty of Engineering and a full professor. He lead the signal processing and communication tracks from 2002 to 2016. In 2009 he spent his sabbatical at Delft University of Technology and Stanford University. Prof. Leshem was an associate editor on IEEE Transactions on Signal Processing 2008-2011, and is currently associate editor for the IEEE Transactions on Signal and Information Processing over Networks. He was member of the IEEE Technical Committee on Signal Processing for Communications (2010-2016) and currently a member of the IEEE Technical Committee on Signal Processing Theory and Methods. He was the leading guest editor of several special issues of the IEEE Signal Processing Magazine and the IEEE Journal on Selected Topics in Signal Processing. His main research interests include wireless networks, learning over networks, applications of game theory to wireless networks, multichannel communication, dynamic and adaptive spectrum management, statistical signal processing, radio-astronomical imaging, set theory, logic and the foundations of mathematics.